EUROPEAN ORGANIZATION FOR NUCLEAR RESEARCH (CERN)

CERN-PH-EP/2014-243
2014/10/24

CMS-HIG-13-007

Search for a standard model-like Higgs boson in the $\mu^+\mu^-$ and e^+e^- decay channels at the LHC

The CMS Collaboration*

Abstract

A search is presented for a standard model-like Higgs boson decaying to the $\mu^+\mu^-$ or e^+e^- final states based on proton-proton collisions recorded by the CMS experiment at the CERN LHC. The data correspond to integrated luminosities of 5.0 fb^{-1} at a centre-of-mass energy of 7 TeV and 19.7 fb^{-1} at 8 TeV for the $\mu^+\mu^-$ search, and of 19.7 fb^{-1} at 8 TeV for the e^+e^- search. To enhance the sensitivity of the search, events are categorized by topologies according to production process and dilepton invariant mass resolution. Upper limits on the production cross section times branching fraction at the 95% confidence level are reported for Higgs boson masses in the range from 120 to 150 GeV. For a Higgs boson with a mass of 125 GeV decaying to $\mu^+\mu^-$, the observed (expected) upper limit on the production rate is found to be 7.4 ($6.5^{+2.8}_{-1.9}$) times the standard model value. This corresponds to an upper limit on the branching fraction of 0.0016. Similarly, for e^+e^-, an upper limit of 0.0019 is placed on the branching fraction, which is $\approx 3.7 \times 10^5$ times the standard model value. These results, together with recent evidence of the 125 GeV boson coupling to τ-leptons with a larger branching fraction consistent with the standard model, show for the first time that the leptonic couplings of the new boson are not flavour-universal.

Submitted to Physics Letters B

*See Appendix A for the list of collaboration members

1 Introduction

After the discovery of a particle with a mass near 125 GeV [1–3] and properties in agreement, within current experimental uncertainties, with those expected of the standard model (SM) Higgs boson, the next critical question is to understand in greater detail the nature of the newly discovered particle. Answering this question with a reasonable confidence requires measurements of its properties and production rates into final states both allowed and disallowed by the SM. Beyond the standard model (BSM) scenarios may contain additional Higgs bosons, so searches for these additional states constitute another test of the SM [4]. For a Higgs boson mass, m_{H}, of 125 GeV, the SM prediction for the Higgs to $\mu^+\mu^-$ branching fraction, $\mathcal{B}(\mathrm{H} \to \mu^+\mu^-)$, is among the smallest accessible at the CERN LHC, 2.2×10^{-4} [5], while the SM prediction for $\mathcal{B}$ $(\mathrm{H} \to \mathrm{e}^+\mathrm{e}^-)$ of approximately 5×10^{-9} is inaccessible at the LHC. Experimentally, however, $\mathrm{H} \to \mu^+\mu^-$ and $\mathrm{H} \to \mathrm{e}^+\mathrm{e}^-$ are the cleanest of the fermionic decays. The clean final states allow a better sensitivity, in terms of cross section, σ, times branching fraction, $\mathcal{B}$, than $\mathrm{H} \to \tau^+\tau^-$. This means that searches for $\mathrm{H} \to \mu^+\mu^-$ and $\mathrm{H} \to \mathrm{e}^+\mathrm{e}^-$, combined with recent strong evidence for decays of the new boson to $\tau^+\tau^-$ [6], may be used to test if the coupling of the new boson to leptons is flavour-universal or proportional to the lepton mass, as predicted by the SM [7]. In addition, a measurement of the $\mathrm{H} \to \mu^+\mu^-$ decay probes the Yukawa coupling of the Higgs boson to second-generation fermions, an important input in understanding the mechanism of electroweak symmetry breaking in the SM [8, 9]. Deviations from the SM expectation could also be a sign of BSM physics [10, 11]. A previous LHC search for SM $\mathrm{H} \to \mu^+\mu^-$ has been performed by the ATLAS Collaboration and placed a 95% confidence level (CL) upper limit of 7.0 times the rate expected from the SM at 125.5 GeV [12]. The ATLAS Collaboration has also performed a search for BSM $\mathrm{H} \to \mu^+\mu^-$ decays within the context of the minimal supersymmetric standard model [13].

This paper reports on a search for a SM-like Higgs boson decaying to either a pair of muons or electrons ($\mathrm{H} \to \ell^+\ell^-$) in proton-proton collisions recorded by the CMS experiment at the LHC. The $\mathrm{H} \to \mu^+\mu^-$ search is performed on data corresponding to integrated luminosities of $5.0 \pm 0.1\,\mathrm{fb}^{-1}$ at a centre-of-mass energy of 7 TeV and $19.7 \pm 0.5\,\mathrm{fb}^{-1}$ at 8 TeV, while the $\mathrm{H} \to \mathrm{e}^+\mathrm{e}^-$ search is only performed on the 8 TeV data. Results are presented for Higgs boson masses between 120 and 150 GeV. For $m_{\mathrm{H}} = 125$ GeV, the SM predicts 19 (95) $\mathrm{H} \to \mu^+\mu^-$ events at 7 TeV (8 TeV), and $\approx 2 \times 10^{-3}$ $\mathrm{H} \to \mathrm{e}^+\mathrm{e}^-$ events at 8 TeV [14–17].

The $\mathrm{H} \to \ell^+\ell^-$ resonance is sought as a peak in the dilepton mass spectrum, $m_{\ell\ell}$, on top of a smoothly falling background dominated by contributions from Drell–Yan production, $\mathrm{t\bar{t}}$ production, and vector boson pair-production processes. Signal acceptance and selection efficiency are estimated using Monte Carlo (MC) simulations, while the background is estimated by fitting the observed $m_{\ell\ell}$ spectrum in data, assuming a smooth functional form.

Near $m_{\mathrm{H}} = 125$ GeV, the SM predicts a Higgs boson decay width much narrower than the dilepton invariant mass resolution of the CMS experiment. For $m_{\mathrm{H}} = 125$ GeV, the SM predicts the Higgs boson decay width to be 4.2 MeV [15], and experimental results indirectly constrain the width to be <22 MeV at the 95% CL [18]. The experimental resolution depends on the angle of each reconstructed lepton relative to the beam axis. For dimuons, the full width at half maximum (FWHM) of the signal peak ranges from 3.9 to 6.2 GeV (for muons with $|\eta| < 2.1$), while for electrons it ranges from 4.0 to 7.2 GeV (for electrons with $|\eta| < 1.44$ or $1.57 < |\eta| < 2.5$).

The sensitivity of this analysis is increased through an extensive categorization of the events, using kinematic variables to isolate regions with a large signal over background (S/B) ratio from regions with smaller S/B ratios. Separate categories are optimized for the dominant Higgs

boson production mode, gluon-fusion (GF), and the sub-dominant production mode, vector boson fusion (VBF). Higgs boson production in association with a vector boson (VH), while not optimized for, is taken into account in the $H \to \mu^+\mu^-$ analysis. The SM predicts Higgs boson production to be 87.3% GF, 7.1% VBF, and 5.0% VH for $m_H = 125\,\text{GeV}$ at 8 TeV [17]. In addition to $m_{\ell\ell}$, the most powerful variables for discriminating between the Higgs boson signal and the Drell–Yan and $t\bar{t}$ backgrounds are the jet multiplicity, the dilepton transverse-momentum ($p_T^{\ell\ell}$), and the invariant mass of the two largest transverse-momentum jets (m_{jj}). The gluon-gluon initial state of GF production tends to lead to more jet radiation than the quark-antiquark initial state of Drell–Yan production, leading to larger $p_T^{\ell\ell}$ and jet multiplicity. Similarly, VBF production involves a pair of forward-backward jets with a large m_{jj} compared to Drell–Yan plus two-jet or $t\bar{t}$ production. Events are further categorized by their $m_{\ell\ell}$ resolution and the kinematics of the jets.

This paper is organized as follows. Section 2 introduces the CMS detector and event reconstruction, Section 3 describes the $H \to \mu^+\mu^-$ event selection, Section 4 the $H \to \mu^+\mu^-$ selection efficiency, Section 5 details the systematic uncertainties included in the $H \to \mu^+\mu^-$ analysis, Section 6 presents the results of the $H \to \mu^+\mu^-$ search, Section 7 describes the $H \to e^+e^-$ search, and Section 8 provides a summary.

2 CMS detector and event reconstruction

The central feature of the CMS apparatus is a superconducting solenoid of 6 m internal diameter, providing a magnetic field of 3.8 T. Within the superconducting solenoid volume are a silicon pixel and strip tracker, a lead tungstate crystal electromagnetic calorimeter (ECAL), and a brass/scintillator hadron calorimeter (HCAL), each composed of a barrel and two endcap sections. Muons are measured in gas-ionization detectors embedded in the steel flux-return yoke outside the solenoid. Extensive forward calorimetry complements the coverage provided by the barrel and endcap detectors.

The first level of the CMS trigger system, composed of custom hardware processors, uses information from the calorimeters and muon detectors to select the most interesting events in a fixed time interval of less than 4 μs. The high level trigger processor farm further decreases the event rate from at most 100 kHz to less than 1 kHz, before data storage. A more detailed description of the detector as well as the definition of the coordinate system and relevant kinematic variables can be found in Ref. [19].

The CMS offline event reconstruction creates a global event description by combining information from all subdetectors. This combined information then leads to a list of particle-flow (PF) objects [20, 21]: candidate muons, electrons, photons, and hadrons. By combining information from all subdetectors, particle identification and energy estimation performance are improved. In addition, double counting subdetector energy deposits when reconstructing different particle types is eliminated.

Due to the high instantaneous luminosity of the LHC, many proton-proton interactions occur in each bunch crossing. An average of 9 and 21 interactions occur in each bunch crossing for the 7 and 8 TeV data samples, respectively. Most interactions produce particles with relatively low transverse-momentum (p_T), compared to the particles produced in an $H \to \ell^+\ell^-$ signal event. These interactions are termed "pileup", and can interfere with the reconstruction of the high-p_T interaction, whose vertex is identified as the vertex with the largest scalar sum of the squared transverse momenta of the tracks associated with it. All charged PF objects with tracks coming from another vertex are then removed.

Hadronic jets are clustered from reconstructed PF objects with the infrared- and collinear-safe anti-k_T algorithm [22, 23], operated with a size parameter of 0.5. The jet momentum is determined as the vectorial sum of the momenta of all PF objects in the jet, and is found in the simulation to be within 5% to 10% of the true momentum over the whole p_T spectrum of interest and detector acceptance. An offset correction is applied to take into account the extra neutral energy clustered in jets due to pileup. Jet energy corrections are derived from the simulation, and are confirmed by in-situ measurements of the energy balance in dijet, photon plus jet, and Z plus jet (where the Z-boson decays to $\mu^+\mu^-$ or e^+e^-) events [24]. The jet energy resolution is 15% at 10 GeV, 8% at 100 GeV, and 4% at 1 TeV [25]. Additional selection criteria are applied to each event to remove spurious jet-like objects originating from isolated noise patterns in certain HCAL regions.

Matching muons to tracks measured in the silicon tracker results in a relative p_T resolution for muons with $20 < p_T < 100$ GeV of 1.3–2.0% in the barrel and better than 6% in the endcaps. The p_T resolution in the barrel is better than 10% for muons with p_T up to 1 TeV [26]. The mass resolution for $Z \to \mu\mu$ decays is between 1.1% and 1.9% depending on the pseudorapidity of each muon, for $|\eta| < 2.1$. The mass resolution for $Z \to ee$ decays when both electrons are in the ECAL barrel (endcaps) is 1.6% (2.6%) [27].

3 $H \to \mu^+\mu^-$ event selection

Online collection of events is performed with a trigger that requires at least one isolated muon candidate with p_T above 24 GeV in the pseudorapidity range $|\eta| \leq 2.1$. In the offline selection, muon candidates are required to pass the "Tight muon selection" [26] and each muon trajectory is required to have an impact parameter with respect to the primary vertex smaller than 5 mm and 2 mm in the longitudinal and transverse directions, respectively. They must also have $p_T > 15$ GeV and $|\eta| \leq 2.1$.

For each muon candidate, an isolation variable is constructed using the scalar sum of the transverse-momentum of particles, reconstructed as PF objects, within a cone centered on the muon. The boundary of the cone is $\Delta R = \sqrt{(\Delta\eta)^2 + (\Delta\phi)^2} = 0.4$ away from the muon, and the p_T of the muon is not included in the sum. While only charged particles associated with the primary vertex are taken into account, a correction must be applied for contamination from neutral particles coming from pileup interactions. On average, in inelastic proton-proton collisions, neutral pileup particles deposit half as much energy as charged pileup particles. The amount of energy coming from charged pileup particles is estimated as the sum of the transverse momenta of charged tracks originating from vertices other than the primary vertex, but still entering the isolation cone. The neutral pileup energy in the isolation cone is then estimated to be 50% of this value and subtracted from the muon isolation variable. A muon candidate is accepted if the corrected isolation variable is less than 12% of the muon p_T.

To pass the offline selection, events must contain a pair of opposite-sign muon candidates passing the above selection, and the muon which triggered the event is required to have $p_T > 25$ GeV. All combinations of opposite-sign pairs, where one of the muons triggers the event, are considered as dimuon candidates in the dimuon invariant mass distribution analysis. Each pair is effectively treated as a separate event, and referred to as such for the remainder of this paper. Less than 0.1% of the SM Higgs boson events and 0.005% of the background events in each category contain more than one pair of muons.

After selecting events with a pair of isolated opposite-sign muons, events are categorized according to the properties of jets. Jets reconstructed from PF objects are only considered if their

p_T is greater than 30 GeV and $|\eta| < 4.7$. A multivariate analysis (MVA) technique is used to discriminate between jets originating from hard interactions and jets originating from pileup [28].

Dimuon events are classified into two general categories: a 2-jet category and a 0,1-jet category. The 2-jet category requires at least two jets, with $p_T > 40$ GeV for the leading jet and $p_T > 30$ GeV for the subleading jet. A 2-jet event must also have $p_T^{miss} < 40$ GeV, where p_T^{miss} is the magnitude of the vector sum of the transverse momenta of the dimuon and dijet systems. The p_T^{miss} requirement reduces the $t\bar{t}$ contamination in the 2-jet category, since $t\bar{t}$ decays also include missing transverse momentum due to neutrinos. All dimuon events not selected for the 2-jet category are placed into the 0,1-jet category where the signal is produced dominantly by GF.

The 2-jet category is further divided into VBF Tight, GF Tight, and Loose subcategories. The VBF Tight category has a large S/B ratio for VBF produced events. It requires $m_{jj} > 650$ GeV and $|\Delta\eta(jj)| > 3.5$, where $|\Delta\eta(jj)|$ is the absolute value of the difference in pseudorapidity between the two leading jets. For a SM Higgs boson with $m_H = 125$ GeV, 79% of the signal events in this category are from VBF production. Signal events in the 2-jet category that do not pass the VBF Tight criteria mainly arise from GF events, which contain two jets from initial-state radiation. The GF Tight category captures these events by requiring the dimuon transverse momentum ($p_T^{\mu\mu}$) to be greater than 50 GeV and $m_{jj} > 250$ GeV. To further increase the sensitivity of this search, 2-jet events that fail the VBF Tight and GF Tight criteria are still retained in a third subcategory called 2-jet Loose.

In the 0,1-jet category, events are split into two subcategories based on the value of $p_T^{\mu\mu}$. The most sensitive subcategory is 0,1-jet Tight which requires $p_T^{\mu\mu}$ greater than 10 GeV, while the events with $p_T^{\mu\mu}$ less than 10 GeV are placed in the 0,1-jet Loose subcategory. The S/B ratio is further improved by categorizing events based on the dimuon invariant mass resolution as follows. Given the narrow Higgs boson decay width, the mass resolution fully determines the shape of the signal peak. The dimuon mass resolution is dominated by the muon p_T resolution, which worsens with increasing $|\eta|$ [26]. Hence, events are further sorted into subcategories based on the $|\eta|$ of each muon and are labeled as "barrel" muons (B) for $|\eta| < 0.8$, "overlap" muons (O) for $0.8 \leq |\eta| < 1.6$, and "endcap" muons (E) for $1.6 \leq |\eta| < 2.1$. The 0,1-jet dimuon events are then assigned, within the corresponding Tight and Loose categories, to all possible dimuon $|\eta|$ combinations. The dimuon mass resolution for each category is shown in Table 1. Due to the limited size of the data samples, the 2-jet subcategories are not split into further subcategories according to the muon p_T resolution. This leads to a total of fifteen subcategories: three 2-jet subcategories, six 0,1-jet Tight subcategories, and six 0,1-jet Loose subcategories.

4 $H \to \mu^+\mu^-$ event selection efficiency

While the background shape and normalization are obtained from data, the selection efficiency for signal events has to be determined using MC simulation. For the GF and VBF production modes, signal samples are produced using the POWHEG–BOX next-to-leading-order (NLO) generator [29–31] interfaced with PYTHIA 6.4.26 [32] for parton showering. VH samples are produced using HERWIG++ [33] and its integrated implementation of the NLO POWHEG method.

These samples are then passed through a simulation of the CMS detector, based on GEANT4 [34], that has been extensively validated on both 7 and 8 TeV data. This validation includes a comparison of data with MC simulations of the Drell–Yan plus jets and $t\bar{t}$ plus jets backgrounds produced using MADGRAPH [35] interfaced with PYTHIA 6.4.26 for parton showering. In all categories, the simulated $m_{\mu\mu}$ spectra agree well with the data, for $110 < m_{\mu\mu} < 160$ GeV. Scale factors related to muon identification, isolation, and trigger efficiency are applied to each

Table 1: Details regarding each of the $H \to \mu^+\mu^-$ categories. The top half of the table refers to the $5.0 \pm 0.1\,\text{fb}^{-1}$ at 7 TeV, while the bottom half refers to the $19.7 \pm 0.5\,\text{fb}^{-1}$ at 8 TeV. Each row lists the category name, FWHM of the signal peak, acceptance times selection efficiency ($A\epsilon$) for GF, $A\epsilon$ for VBF, $A\epsilon$ for VH, expected number of SM signal events in the category for $m_H = 125\,\text{GeV}$ (N_S), number of background events within a FWHM-wide window centered on 125 GeV estimated by a signal plus background fit to the data (N_B), number of observed events within a FWHM-wide window centered on 125 GeV (N_{Data}), systematic uncertainty to account for the parameterization of the background (N_P), and N_P divided by the statistical uncertainty on the fitted number of signal events (N_P/σ_{Stat}). The expected number of SM signal events is $N_S = \mathcal{L} \times (\sigma\mathcal{B}A\epsilon)_{GF} + \mathcal{L} \times (\sigma\mathcal{B}A\epsilon)_{VBF} + \mathcal{L} \times (\sigma\mathcal{B}A\epsilon)_{VH}$, where $\mathcal{L}$ is the integrated luminosity and $\sigma\mathcal{B}$ is the SM cross section times branching fraction.

	FWHM	$A\epsilon$ [%]							N_P/σ_{Stat}
Category	[GeV]	GF	VBF	VH	N_S	N_B	N_{Data}	N_P	[%]
0,1-jet Tight BB	3.4	9.7	8.1	8.9	1.83	226.4	245	22.5	101
0,1-jet Tight BO	4.0	14.0	11.0	13.0	2.56	470.3	459	42.4	121
0,1-jet Tight BE	4.4	4.9	3.8	4.8	0.92	234.8	235	16.6	65
0,1-jet Tight OO	4.8	5.2	3.9	4.9	0.97	226.5	236	11.5	52
0,1-jet Tight OE	5.3	4.0	3.0	4.2	0.75	237.5	228	26.5	106
0,1-jet Tight EE	5.9	0.9	0.7	1.0	0.17	71.4	57	11.4	97
0,1-jet Loose BB	3.2	2.2	0.1	0.1	0.38	151.4	127	17.2	95
0,1-jet Loose BO	3.9	3.1	0.2	0.2	0.52	307.0	291	18.9	71
0,1-jet Loose BE	4.2	1.2	0.1	0.1	0.20	148.7	178	19.1	102
0,1-jet Loose OO	4.5	1.2	0.1	0.1	0.20	144.7	143	19.1	113
0,1-jet Loose OE	5.1	1.0	0.1	0.1	0.16	160.1	159	16.1	75
0,1-jet Loose EE	5.8	0.2	0.0	0.0	0.03	41.6	39	5.6	51
2-jet VBF Tight	4.4	0.1	8.7	0.0	0.14	1.3	2	0.5	24
2-jet GF Tight	4.5	0.5	7.9	0.5	0.20	12.9	16	1.7	27
2-jet Loose	4.3	2.1	6.2	10.2	0.53	66.2	78	8.4	64
Sum of categories	—	50.3	53.9	48.1	9.56	2500.8	2493	—	—
0,1-jet Tight BB	3.9	9.6	7.1	8.5	8.87	1208.0	1311	40.8	73
0,1-jet Tight BO	4.4	13.0	10.0	13.0	12.45	2425.3	2474	102.2	127
0,1-jet Tight BE	4.7	4.9	3.4	4.6	4.53	1204.8	1212	63.8	111
0,1-jet Tight OO	5.0	5.3	3.6	5.0	4.90	1112.7	1108	39.0	71
0,1-jet Tight OE	5.5	4.1	2.8	4.2	3.85	1162.1	1201	151.1	251
0,1-jet Tight EE	6.4	0.9	0.6	1.1	0.85	350.8	323	34.2	107
0,1-jet Loose BB	3.7	2.1	0.1	0.1	1.73	715.4	697	40.2	94
0,1-jet Loose BO	4.3	2.9	0.2	0.2	2.41	1436.4	1432	85.5	158
0,1-jet Loose BE	4.5	1.1	0.1	0.1	0.90	725.9	782	74.9	166
0,1-jet Loose OO	4.9	1.1	0.1	0.1	0.96	727.4	686	33.2	74
0,1-jet Loose OE	5.5	0.9	0.1	0.1	0.76	791.8	832	78.2	158
0,1-jet Loose EE	6.2	0.2	0.0	0.0	0.18	218.5	209	18.9	87
2-jet VBF Tight	5.0	0.2	11.0	0.0	0.95	10.6	8	1.6	35
2-jet GF Tight	5.1	0.7	8.4	0.6	1.14	74.8	76	11.8	88
2-jet Loose	4.7	2.4	6.3	10.4	2.90	431.7	387	25.3	73
Sum of categories	—	49.4	53.8	48.0	47.38	12596.2	12738	—	—

simulated signal sample to correct for discrepancies between the detector simulation and data. These scale factors are estimated using the "tag-and-probe" technique [26]. The detector simulation and data typically agree to within 1% on the muon identification efficiency, to within 2% on the muon isolation efficiency, and to within 5% on the muon trigger efficiency.

The overall acceptance times selection efficiency for the $H \to \mu^+\mu^-$ signal depends on the mass of the Higgs boson. For a Higgs boson mass of 125 GeV, the acceptance times selection efficiencies are shown in Table 1.

5 $H \to \mu^+\mu^-$ systematic uncertainties

Since the statistical analysis is performed on the dimuon invariant mass spectrum, it is necessary to categorize the sources of systematic uncertainties into "shape" uncertainties that change the shape of the dimuon invariant mass distribution, and "rate" uncertainties that affect the overall signal yield in each category.

The only relevant shape uncertainties for the signal are related to the knowledge of the muon momentum scale and resolution and they affect the width of the signal peak by 3%. The signal shape is parameterized by a double-Gaussian (see Section 6) and this uncertainty is applied by constraining the width of the narrower Gaussian. The probability density function used to constrain this nuisance parameter in the limit setting procedure is itself Gaussian with its mean set to the nominal value and its width set to 3% of the nominal value.

Rate uncertainties in the signal yield are evaluated separately for each Higgs boson production process and each centre-of-mass energy. These uncertainties are applied using log-normal probability density functions as described in Ref. [36].

To estimate the theoretical uncertainty in the signal production processes due to neglected higher-order quantum corrections, the renormalization and factorization scales are varied simultaneously by a factor of two up and down from their nominal values. This leads to an uncertainty in the cross section and acceptance times efficiency which depends on the mass of the Higgs boson. For 125 GeV GF production, the uncertainty in the signal yield ranges from 1% in the 0,1-jet Tight category to 25% in the 2-jet VBF Tight and GF Tight categories [15–17]. For VBF production, the uncertainties range from 1% to 7% [15–17].

Uncertainty in the knowledge of the parton distribution functions (PDFs) also leads to uncertainty in the signal production process. This uncertainty is estimated using the PDF4LHC prescription [37, 38] and the CT10 [39], MSTW2008 [40], and NNPDF 2.3 [41] PDF sets provided by the LHAPDF package version 5.8.9 [42]. The value of the uncertainty depends on the mass of the Higgs boson. For $m_H = 125$ GeV, the uncertainties on the signal yields for GF and VBF are 11% and 5%, respectively [15–17].

For VH production, only rate uncertainties in the production cross section due to quantum corrections and PDFs are considered. They are 3% or less.

Uncertainty in the modeling of the parton showers and underlying event activity may affect the kinematics of selected jets. This uncertainty is estimated by comparing various tunes of the relevant PYTHIA parameters. The D6T [43], P0 [44], ProPT0, and ProQ20 [45] tunes are compared with the Z2* [43] tune, which is the nominal choice. Signal yield uncertainties range from 6% to 60% (the largest uncertainty is in the 2-jet VBF Tight category) for the GF production mode and 2% to 15% for the VBF production mode in the various categories. Large uncertainties in the 2-jet categories are expected for the GF production mode, since two-jet events are simulated

solely by parton showering in the POWHEG–PYTHIA NLO samples.

The theoretical uncertainty in the branching fraction to $\mu^+\mu^-$ is taken from Refs. [15–17], and depends on the Higgs boson mass. For $m_{\mathrm{H}} = 125\,\mathrm{GeV}$, it is 6%, while it shrinks to 3% for $m_{\mathrm{H}} = 150\,\mathrm{GeV}$.

The uncertainty in the luminosity, 2.2% at 7 TeV [46] and 2.6% at 8 TeV [47], is directly applied to the signal yield in all categories. The signal yield uncertainty due to the limited size of the simulated event samples varies from 1% to 8% depending on the category.

The small uncertainty associated with the "tag-and-probe" technique used to determine the data to simulation muon efficiency scale factors leads to an uncertainty in the signal yield of 1.6% [26].

A systematic uncertainty in the knowledge of the pileup multiplicity is evaluated by varying the total cross section for inelastic proton-proton collisions. The resulting uncertainty in the signal yield varies, for GF production, from less than 1% to 5% in the various categories, while for VBF production it varies from less than 1% to 2%.

The acceptance and selection efficiency of the jet-based selections are affected by uncertainty in the jet energy resolution and absolute jet energy scale calibration [24]. The energy resolution related uncertainty in the signal yield is 1% to 3% for GF and 1% to 2% for VBF, while the absolute energy scale calibration uncertainty in the signal yield is 1% to 8% for GF, and 2% to 6% for VBF in the various categories.

Misidentification of "hard jets" (jets originating from the hard interaction) as "pileup jets" (jets originating from pileup interactions) can lead to migration of signal events from the 2-jet category to the 0,1-jet category. Events containing a Z-boson, tagged by its dilepton decay, recoiling against a jet provide a pure source of hard jets similar to the Higgs boson signal. Data events may then be used to estimate the misidentification rate of the MVA technique used to discriminate between hard jets and pileup jets using data [28]. A pure source of hard jets is found by selecting events with $p_{\mathrm{T}}^{\mathrm{Z}} > 30\,\mathrm{GeV}$ and jets where $|\Delta\phi(Z,\mathrm{j})| > 2.5$ and $0.5 < p_{\mathrm{T}}^{\mathrm{j}}/p_{\mathrm{T}}^{\mathrm{Z}} < 1.5$ The misidentification rate of these jets as pileup jets is compared in data and simulation, and the difference taken as a systematic uncertainty. The resulting uncertainty in the signal yield varies from 1% to 4% for the various categories.

When estimating each of the signal yield uncertainties, attention is paid to the sign of the yield variation in each category. Categories that vary in the same direction are considered fully correlated while categories that vary in opposite directions are considered anticorrelated. These correlations are considered between all categories at both beam energies for all of the signal yield uncertainties except for the luminosity uncertainty and the uncertainty caused by the limited size of the simulated event samples. The luminosity uncertainty is considered fully correlated between all categories, but uncorrelated between the two centre-of-mass energies. The MC simulation statistical uncertainty is considered uncorrelated between all categories and both centre-of-mass energies.

To account for the possibility that the nominal background parameterization may imperfectly describe the true background shape, an additional systematic uncertainty is included. This uncertainty is implemented as a floating additive contribution to the number of signal events, constrained by a Gaussian probability density function with mean set to zero and width set to the systematic uncertainty. This systematic uncertainty is estimated by checking the bias in terms of the number of signal events that are found when fitting the signal plus nominal background model (see Section 6) to pseudo-data generated from various alternative background

models, including polynomials, that were fit to data. Bias estimates are performed for Higgs boson mass points from 120 to 150 GeV. The uncertainty estimate is then taken as the maximum absolute value of the bias of all of the mass points and all of the alternative background models. It is then applied uniformly to all Higgs boson masses. The estimates of the uncertainty in the parameterization of the background (N_P) are shown in Table 1 for each category. The effect of this systematic uncertainty is larger than all of the others. The expected limit (see Section 6) would be 20% lower at $m_H = 125$ GeV without the systematic uncertainty in the parameterization of the background.

6 $H \to \mu^+\mu^-$ results

To estimate the signal rate, the dimuon invariant mass ($m_{\mu\mu}$) spectrum is fit with the sum of parameterized signal and background shapes. This fit is performed simultaneously in all of the categories. Since in the mass range of interest the natural width of the Higgs boson is narrower than the detector resolution, the $m_{\mu\mu}$ shape is only dependent on the detector resolution and QED final state radiation. A double-Gaussian function is chosen to parameterize the shape of the signal. The background shape, dominated by the Drell–Yan process, is modeled by a function, $f(m_{\mu\mu})$, that is the sum of a Breit–Wigner function and a $1/m_{\mu\mu}^2$ term, to model the Z-boson and photon contributions, both multiplied by an exponential function to approximate the effect of the PDF on the $m_{\mu\mu}$ distribution. This function is shown in the following equation, and involves the parameters λ, β, m_Z, and Γ:

$$f(m_{\mu\mu}) = \beta C_1 e^{-\lambda m_{\mu\mu}} \frac{1}{(m_{\mu\mu} - m_Z)^2 + \frac{\Gamma^2}{4}} + (1-\beta) C_2 e^{-\lambda m_{\mu\mu}} \frac{1}{m_{\mu\mu}^2}. \quad (1)$$

The coefficients C_1 and C_2 are set to ensure the integral of each of the two terms is normalized to unity in the $m_{\mu\mu}$ fit range, 110 to 160 GeV. Before results are extracted, the mass and width of the Z-boson peak, m_Z and Γ, are estimated by fitting a Breit–Wigner function to the Z-boson mass peak region (88–94 GeV) in each category. The other parameters, λ and β, are fit simultaneously with the amount of signal in the signal plus background fit. Besides the Drell–Yan process, most of the remaining background events come from $t\bar{t}$ production. The background parameterization has been shown to fit the dimuon mass spectrum well, even when it includes a large $t\bar{t}$ fraction. Fits of the background model to data (assuming no signal contribution) are presented in Fig. 1 for the most sensitive categories: the 0,1-jet Tight category with both muons reconstructed in the barrel region and the 2-jet VBF Tight category.

Results are presented in terms of the signal strength, which is the ratio of the observed (or expected) $\sigma\mathcal{B}$, to that predicted in the SM for the $H \to \mu^+\mu^-$ process. Results are also presented, for $m_H = 125$ GeV, in terms of $\sigma\mathcal{B}$, and $\mathcal{B}$. No significant excess is observed. Upper limits at the 95% CL are presented using the CL_s criterion [48, 49]. They are calculated using an asymptotic profile likelihood ratio method [36, 50, 51] involving dimuon mass shapes for each signal process and for background. Systematic uncertainties are incorporated as nuisance parameters and treated according to the frequentist paradigm [36].

Exclusion limits for Higgs boson masses from 120 to 150 GeV are shown in Fig. 2. The observed 95% CL upper limits on the signal strength at 125 GeV are 22.4 using the 7 TeV data and 7.0 using the 8 TeV data. The corresponding background-only expected limits are $16.6^{+7.3}_{-4.9}$ using the 7 TeV data and $7.2^{+3.2}_{-2.1}$ using the 8 TeV data. Accordingly, the combined observed limit for 7 and 8 TeV is 7.4, while the background-only expected limit is $6.5^{+2.8}_{-1.9}$. The best fit value of the signal strength for a Higgs boson mass of 125 GeV is $0.8^{+3.5}_{-3.4}$. We did not restrict the fit to positive values, to preserve the generality of the result.

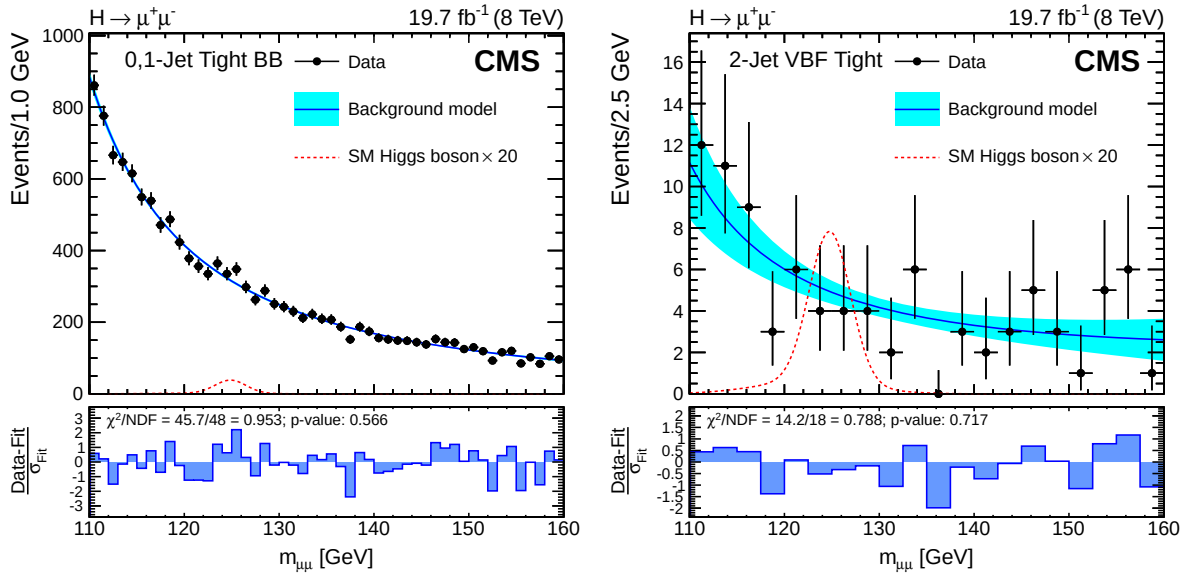

Figure 1: The dimuon invariant mass at 8 TeV and the background model are shown for the 0,1-jet Tight category when both muons are reconstructed in the barrel (left) and the 2-jet VBF Tight category (right). A best fit of the background model (see text) is shown by a solid line, while its fit uncertainty is represented by a lighter band. The dotted line illustrates the expected SM Higgs boson signal enhanced by a factor of 20, for $m_{\mathrm{H}} = 125\,\mathrm{GeV}$. The lower histograms show the residual for each bin (Data-Fit) normalized by the Poisson statistical uncertainty of the background model (σ_{Fit}). Also given are the sum of squares of the normalized residuals (χ^2) divided by the number of degrees of freedom (NDF) and the corresponding p-value assuming the sum follows the χ^2 distribution.

Exclusion limits in terms of $\sigma(8\,\text{TeV})\mathcal{B}$ using only 8 TeV data are shown in Fig. 3 (left). The relative contributions of GF, VBF, and VH are assumed to be as predicted in the SM, and theoretical uncertainties on the cross sections and branching fractions are omitted. At 125 GeV, the observed 95% CL upper limit on $\sigma(7\,\text{TeV})\mathcal{B}$ using only 7 TeV data is 0.084 pb, while the background-only expected limit is $0.062^{+0.026}_{-0.018}$ pb. Using only 8 TeV data, the observed limit on $\sigma(8\,\text{TeV})\mathcal{B}$ is 0.033 pb, while the background-only expected limit is $0.034^{+0.014}_{-0.010}$ pb. To combine 7 and 8 TeV data, the SM ratio of production cross sections is assumed and the result is quoted at a reference energy of 8 TeV. This leads to an observed limit of 0.035 pb on $\sigma(8\,\text{TeV})\mathcal{B}$ and a background-only expected limit of $0.031^{+0.013}_{-0.010}$ pb. Assuming the SM production cross section, this corresponds to an upper limit on $\mathcal{B}(H \to \mu^+\mu^-)$ of 0.0016.

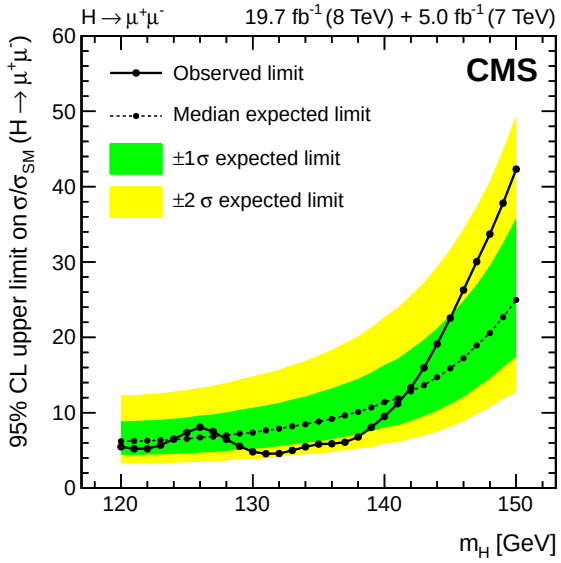

Figure 2: Mass scan for the background-only expected and observed combined exclusion limits.

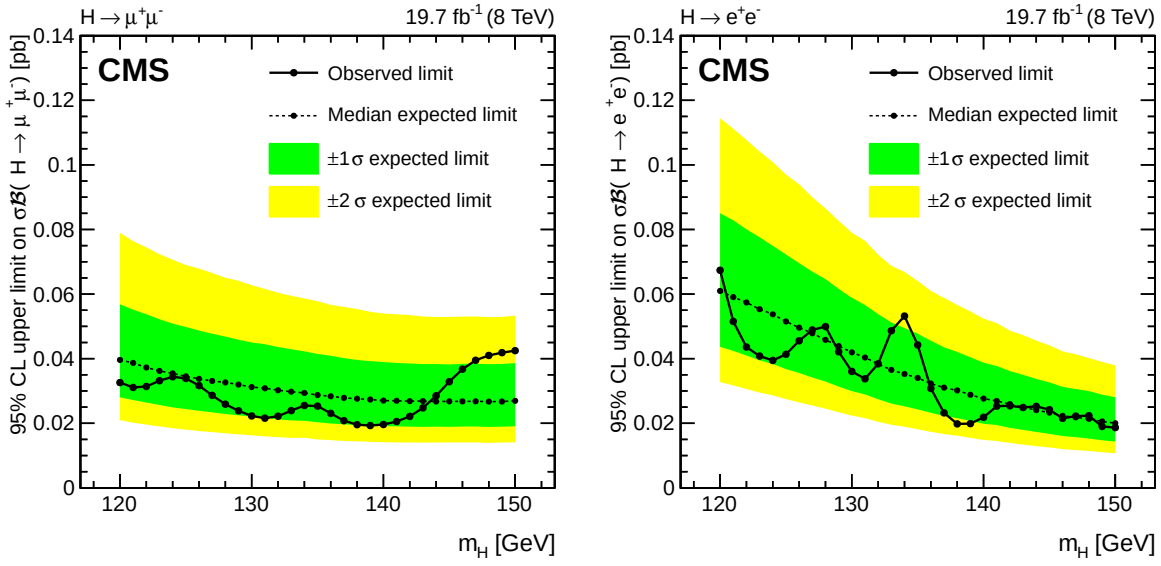

Figure 3: Exclusion limits on $\sigma\mathcal{B}$ are shown for $H \to \mu^+\mu^-$ (left), and for $H \to e^+e^-$ (right), both for 8 TeV. Theoretical uncertainties on the cross sections and branching fraction are omitted, and the relative contributions of GF, VBF, and VH are as predicted in the SM.

Exclusion limits on individual production modes may also be useful to constrain BSM models

that predict $H \to \mu^+\mu^-$ production dominated by a single mode. Limits are presented on the signal strength and $\sigma\mathcal{B}$ using a combination of 7 and 8 TeV data. The limits on $\sigma\mathcal{B}$ are at a reference energy of 8 TeV assuming the SM ratio of production cross sections. The observed 95% CL upper limit on the GF signal strength, assuming the VBF and VH rates are zero, is 13.2, while the background-only expected limit is $9.8^{+4.4}_{-2.9}$. This corresponds to an observed upper limit on $\sigma_{\mathrm{GF}}(8\,\mathrm{TeV})\mathcal{B}$ of 0.054 pb and an expected limit of $0.041^{+0.017}_{-0.012}$ pb. Similarly, the observed upper limit on the VBF signal strength, assuming the GF and VH rates are zero, is 11.2, while the background-only expected limit is $13.4^{+6.6}_{-4.2}$. This corresponds to an observed upper limit on $\sigma_{\mathrm{VBF}}(8\,\mathrm{TeV})\mathcal{B}$ of 0.0038 pb and an expected limit of $0.0046^{+0.0023}_{-0.0015}$ pb.

For $m_{\mathrm{H}} = 125\,\mathrm{GeV}$, an alternative $H \to \mu^+\mu^-$ analysis was performed to check the results of the main analysis. It uses an alternative muon isolation variable based only on tracker information, an alternative jet reconstruction algorithm (the jet-plus-track algorithm [52]), and an alternative event categorization. The event categorization contains similar 2-jet categories to the main analysis, while separate categories are utilized for 0-jet and 1-jet events. Dimuon mass resolution-based categories are not used, but the 0-jet category does contain two subcategories separated by $p_{\mathrm{T}}^{\mu\mu}$. As in the main analysis, results are extracted by fitting signal and background shapes to the $m_{\mu\mu}$ spectra in each category, but unlike the main analysis, $f(m_{\mu\mu}) = \exp(p_1 m_{\mu\mu})/(m_{\mu\mu} - p_2)^2$ is used as the background shape. The systematic uncertainty on the parameterization of the background is estimated and applied in the same way as in the main analysis. For the alternative analysis, the observed (expected) 95% CL upper limit on the signal strength is 7.8 ($6.5^{+2.8}_{-1.9}$) for the combination of 7 TeV and 8 TeV data and $m_{\mathrm{H}} = 125\,\mathrm{GeV}$. The observed limits of both the main and alternative analyses are within one standard deviation of their respective background-only expected limits, for $m_{\mathrm{H}} = 125\,\mathrm{GeV}$.

7 Search for Higgs boson decays to e^+e^-

In the SM, the branching fraction of the Higgs boson into e^+e^- is tiny, because the fermionic decay width is proportional to the mass of the fermion squared. This leads to poor sensitivity to SM production for this search when compared to the search for $H \to \mu^+\mu^-$. On the other hand, the sensitivity in terms of $\sigma\mathcal{B}$ is similar to $H \to \mu^+\mu^-$, because dielectrons and dimuons share similar invariant mass resolutions, selection efficiencies, and backgrounds. Since the sensitivity to the SM rate of $H \to e^+e^-$ is so poor, an observation of the newly discovered particle decaying to e^+e^- with the current integrated luminosity would be evidence of physics beyond the standard model.

In a similar way to the $H \to \mu^+\mu^-$ analysis, a search in the m_{ee} spectrum is performed for a narrow peak over a smoothly falling background. The irreducible background is dominated by Drell–Yan production, with smaller contributions from $t\bar{t}$ and diboson production. Misidentified electrons make up a reducible background that is highly suppressed by the electron identification criteria. The reducible $H \to \gamma\gamma$ background is estimated from simulation to be negligible compared to other backgrounds, although large compared to the SM $H \to e^+e^-$ signal. The overall background shape and normalization are estimated by fitting the observed m_{ee} spectrum in data, assuming a smooth functional form, while the signal acceptance times selection efficiency is estimated from simulation. The analysis is performed only on proton-proton collision data collected at 8 TeV, corresponding to an integrated luminosity of $19.7 \pm 0.5\,\mathrm{fb}^{-1}$.

The trigger selection requires two electrons, one with transverse energy, E_{T}, greater than 17 GeV and the other with E_{T} greater than 8 GeV. These electrons are required to be isolated with respect to additional energy deposits in the ECAL, and to pass selections on the ECAL cluster

shape. In the offline selection, electrons are required to be inside the ECAL fiducial region: $|\eta| < 1.44$ (barrel) or $1.57 < |\eta| < 2.5$ (endcaps). Their energy is estimated by the same multivariate regression technique used in the CMS $H \to ZZ$ analysis [53], and their E_T is required to be greater than 25 GeV. Electrons are also required to satisfy standard CMS identification and isolation requirements, which correspond to a single electron efficiency of around 90% in the barrel and 80% in the endcaps [54].

To improve the sensitivity of the search we separate the sample into four distinct categories: two 0,1-jet categories and two for which a pair of jets is required. The two 2-jet categories are designed to select events produced via the VBF process. The two jets are required to have an invariant mass greater than 500 (250) GeV for the 2-jet Tight (Loose) category, $p_T > 30\,(20)$ GeV, $|\Delta\eta(jj)| > 3.0$, $|\Delta\phi(jj, e^+e^-)| > 2.6$, and $|z| = |\eta(e^+e^-) - [\eta(j_1) + \eta(j_2)]/2| < 2.5$ [55]. The cut on z ensures that the dielectron is produced centrally in the dijet reference frame, which helps to enhance the VBF signal over the Drell–Yan background. More details on the selection can be found in Ref. [56]. The rest of the events are classified into two 0,1-jet categories. To exploit the better energy resolution of electrons in the barrel region, these categories are defined as: both electrons in the ECAL barrel (0,1-jet BB) or at least one of them in the endcap (0,1-jet Not BB). For each category, the FWHM of the expected signal peak, expected number of SM signal events for $m_H = 125$ GeV, acceptance times selection efficiency, number of background events near 125 GeV, and number of data events near 125 GeV are shown in Table 2.

Data have been compared to the simulated Drell–Yan and $t\bar{t}$ background samples described in Section 4. In all categories, the dielectron invariant mass spectra from 110 to 160 GeV agree well, and the normalizations agree within 4.5%. Using simulation, the reducible background of $H \to \gamma\gamma$ events has also been estimated. For $m_H = 125$ GeV, 0.23 SM $H \to \gamma\gamma$ events are expected to pass the dielectron selection compared to about 10^{-3} events for the SM $H \to e^+e^-$ signal. While this background is much larger than the SM $H \to e^+e^-$ signal, it is negligible compared to the Drell–Yan and $t\bar{t}$ backgrounds in each category.

Results are extracted from the data for m_H values between 120 and 150 GeV by fitting the mass spectra of the four categories in the range $110 < m_{ee} < 160$ GeV. The parameterization used for the background is the same as used in the $\mu^+\mu^-$ search, Equation (1). Background-only m_{ee} fits to data are shown in Fig. 4 for the 0,1-jet BB and 2-jet Tight categories.

The uncertainty related to the choice of background parameterization is estimated and incorporated into the results using the same method as in the $\mu^+\mu^-$ search (see Section 5). This uncertainty in terms of the number of signal events (N_P) is shown in Table 2. This systematic uncertainty is larger than all of the others, and removing it would lower the expected limit by 28%, for $m_H = 125$ GeV.

Systematic uncertainties on the electron trigger and identification efficiencies lead to signal yield uncertainties of 1% and 2%, respectively. The uncertainty in the jet energy resolution and jet energy calibration result in an uncertainty in the signal yield of <1% (2%) for GF (VBF) in the 0,1-jet categories and 11% (3%) for GF (VBF) in the 2-jet categories. Uncertainties in the knowledge of the integrated luminosity, modeling of parton-showers, modeling of underlying event activity, neglected higher-order quantum corrections, and knowledge of the PDFs are identical to that of $H \to \mu^+\mu^-$ described in Section 5.

The uncertainties on the electron trigger efficiency, electron identification efficiency, integrated luminosity, neglected higher-order quantum corrections, and PDFs are considered fully correlated between the four categories. The signal yield uncertainties due to the modeling of parton showers, underlying event activity, jet energy resolution, and jet energy calibration primarily

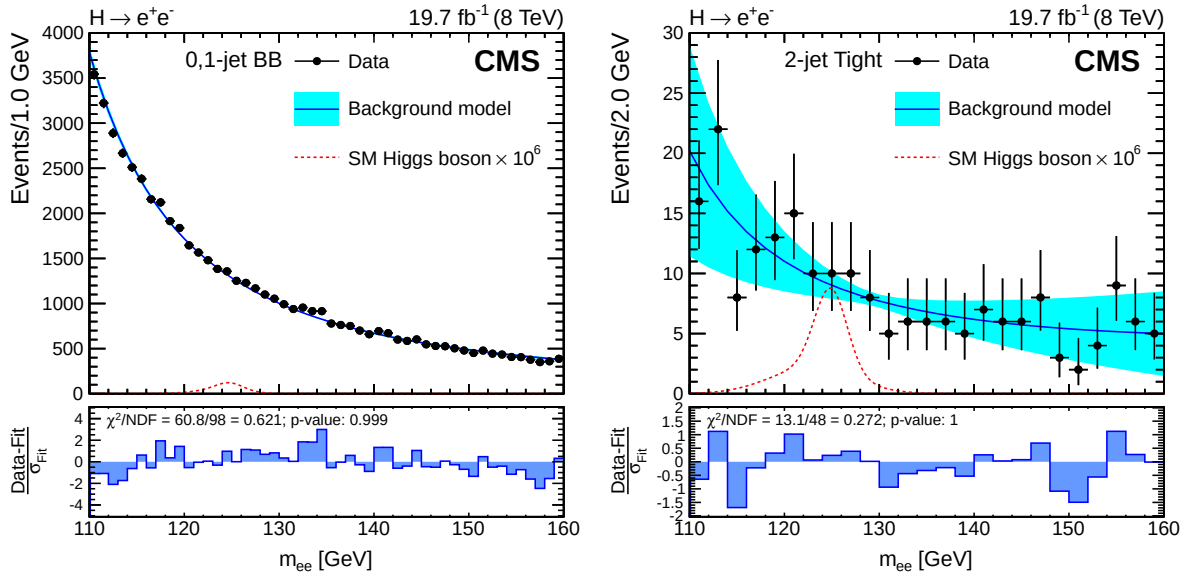

Figure 4: The dielectron invariant mass at 8 TeV and the background model are shown for the 0,1-jet BB (left) and 2-jet Tight (right) categories. A best fit of the background model (see Section 6) is shown by a solid line, while its fit uncertainty is represented by a lighter band. The dotted line illustrates the expected SM Higgs boson signal enhanced by a factor of 10^6, for $m_{\mathrm{H}} = 125$ GeV. The lower histograms show the residual for each bin (Data-Fit) normalized by the Poisson statistical uncertainty of the background model (σ_{Fit}). Also given are the sum of squares of the normalized residuals (χ^2) divided by the number of degrees of freedom (NDF) and the corresponding p-value assuming the sum follows the χ^2 distribution.

affect the jet selection and lead to event migration between the 0,1-jet and 2-jet categories. As a result, they are considered fully anticorrelated between the 0,1-jet categories and the 2-jet categories.

No significant excess of events is observed. Upper limits on $\sigma(8\,\mathrm{TeV})\mathcal{B}$ and $\mathcal{B}$ are reported. The observed 95% CL upper limit on $\sigma(8\,\mathrm{TeV})\mathcal{B}$ at 125 GeV is 0.041 pb while the background-only expected limit is $0.052^{+0.022}_{-0.015}$ pb. Assuming the SM production cross-section, this corresponds to an observed upper limit on $\mathcal{B}(\mathrm{H} \to \mathrm{e}^+\mathrm{e}^-)$ of 0.0019, which is approximately 3.7×10^5 times the SM prediction. Upper limits on $\sigma(8\,\mathrm{TeV})\mathcal{B}$ are shown for Higgs boson masses from 120 to 150 GeV at the 95% CL in Fig. 3 (right).

8 Summary

Results are presented from a search for a SM-like Higgs boson decaying to $\mu^+\mu^-$ and for the first time to $\mathrm{e}^+\mathrm{e}^-$. For the search in $\mu^+\mu^-$, the analyzed CMS data correspond to integrated luminosities of $5.0 \pm 0.1\,\mathrm{fb}^{-1}$ collected at 7 TeV and $19.7 \pm 0.5\,\mathrm{fb}^{-1}$ collected at 8 TeV, while only the 8 TeV data are used for the search in the $\mathrm{e}^+\mathrm{e}^-$ channel. The Higgs boson signal is sought as a narrow peak in the dilepton invariant mass spectrum on top of a smoothly falling background dominated by the Drell–Yan, $\mathrm{t\bar{t}}$, and vector boson pair-production processes. Events are split into categories corresponding to different production topologies and dilepton invariant mass resolutions. The signal strength is then extracted using a simultaneous fit to the dilepton invariant mass spectra in all of the categories.

No significant $\mathrm{H} \to \mu^+\mu^-$ signal is observed. Upper limits are set on the signal strength at the 95% CL. Results are presented for Higgs boson masses between 120 and 150 GeV. The com-

Table 2: Details regarding each category of the $H \to e^+e^-$ analysis, for $19.7 \pm 0.5\,fb^{-1}$ at 8 TeV. Each row lists the category name, FWHM of the signal peak, acceptance times selection efficiency ($A\epsilon$) for GF, $A\epsilon$ for VBF, expected number of SM signal events in the category times 10^5 for $m_H = 125\,GeV$ (N_S), number of background events within a FWHM-wide window centered on 125 GeV estimated by a signal plus background fit to the data (N_B), number of observed events within a FWHM-wide window centered on 125 GeV (N_{Data}), systematic uncertainty to account for the parameterization of the background (N_P), and N_P divided by the statistical uncertainty on the fitted number of signal events (N_P/σ_{Stat}). The expected number of SM signal events is $N_S = \mathcal{L} \times (\sigma\mathcal{B}A\epsilon)_{GF} + \mathcal{L} \times (\sigma\mathcal{B}A\epsilon)_{VBF}$, where $\mathcal{L}$ is the integrated luminosity and $\sigma\mathcal{B}$ is the SM cross section times branching fraction.

	FWHM	$A\epsilon$ [%]						N_P/σ_{Stat}
Category	[GeV]	GF	VBF	$N_S \times 10^5$	N_B	N_{Data}	N_P	[%]
0,1-jet BB	4.0	27.5	16.7	56.1	5208.9	5163	75.0	61
0,1-jet Not BB	7.1	17.0	9.7	34.6	8675.0	8748	308.7	174
2-jet Tight	3.8	0.5	10.7	2.6	17.7	22	19.5	71
2-jet Loose	4.7	1.0	7.3	3.1	79.5	84	43.2	88
Sum of categories	—	46.0	44.4	96.4	13981.1	14017	—	—

bined observed limit on the signal strength, for a Higgs boson with a mass of 125 GeV, is 7.4, while the expected limit is $6.5^{+2.8}_{-1.9}$. Assuming the SM production cross section, this corresponds to an upper limit of 0.0016 on $\mathcal{B}(H \to \mu^+\mu^-)$. For a Higgs boson mass of 125 GeV, the best fit signal strength is $0.8^{+3.5}_{-3.4}$.

In the $H \to e^+e^-$ channel, SM Higgs boson decays are far too rare to detect, and no signal is observed. For a Higgs boson mass of 125 GeV, a 95% CL upper limit of 0.041 pb is set on $\sigma\mathcal{B}(H \to e^+e^-)$ at 8 TeV. Assuming the SM production cross section, this corresponds to an upper limit on $\mathcal{B}(H \to e^+e^-)$ of 0.0019, which is approximately 3.7×10^5 times the SM prediction. For comparison, the $H \to \mu^+\mu^-$ observed 95% CL upper limit on $\sigma\mathcal{B}(H \to \mu^+\mu^-)$ is 0.033 pb (using only 8 TeV data), which is 7.0 times the expected SM Higgs boson cross section.

These results, together with recent evidence for the 125 GeV boson's coupling to τ-leptons [6] with a larger $\mathcal{B}$ consistent with the SM value of 0.0632 ± 0.0036 [5], show for the first time that the leptonic couplings of the new boson are not flavour-universal, confirming the SM prediction.

Acknowledgments

We congratulate our colleagues in the CERN accelerator departments for the excellent performance of the LHC and thank the technical and administrative staffs at CERN and at other CMS institutes for their contributions to the success of the CMS effort. In addition, we gratefully acknowledge the computing centres and personnel of the Worldwide LHC Computing Grid for delivering so effectively the computing infrastructure essential to our analyses. Finally, we acknowledge the enduring support for the construction and operation of the LHC and the CMS detector provided by the following funding agencies: BMWFW and FWF (Austria); FNRS and FWO (Belgium); CNPq, CAPES, FAPERJ, and FAPESP (Brazil); MES (Bulgaria); CERN; CAS, MoST, and NSFC (China); COLCIENCIAS (Colombia); MSES and CSF (Croatia); RPF (Cyprus); MoER, ERC IUT and ERDF (Estonia); Academy of Finland, MEC, and HIP (Finland); CEA and CNRS/IN2P3 (France); BMBF, DFG, and HGF (Germany); GSRT (Greece); OTKA and NIH (Hungary); DAE and DST (India); IPM (Iran); SFI (Ireland); INFN (Italy); NRF and WCU (Republic of Korea); LAS (Lithuania); MOE and UM (Malaysia); CINVESTAV, CONACYT, SEP,

and UASLP-FAI (Mexico); MBIE (New Zealand); PAEC (Pakistan); MSHE and NSC (Poland); FCT (Portugal); JINR (Dubna); MON, RosAtom, RAS and RFBR (Russia); MESTD (Serbia); SEIDI and CPAN (Spain); Swiss Funding Agencies (Switzerland); MST (Taipei); ThEPCenter, IPST, STAR and NSTDA (Thailand); TUBITAK and TAEK (Turkey); NASU and SFFR (Ukraine); STFC (United Kingdom); DOE and NSF (USA).

Individuals have received support from the Marie-Curie programme and the European Research Council and EPLANET (European Union); the Leventis Foundation; the A. P. Sloan Foundation; the Alexander von Humboldt Foundation; the Belgian Federal Science Policy Office; the Fonds pour la Formation à la Recherche dans l'Industrie et dans l'Agriculture (FRIA-Belgium); the Agentschap voor Innovatie door Wetenschap en Technologie (IWT-Belgium); the Ministry of Education, Youth and Sports (MEYS) of the Czech Republic; the Council of Science and Industrial Research, India; the HOMING PLUS programme of Foundation for Polish Science, cofinanced from European Union, Regional Development Fund; the Compagnia di San Paolo (Torino); the Consorzio per la Fisica (Trieste); MIUR project 20108T4XTM (Italy); the Thalis and Aristeia programmes cofinanced by EU-ESF and the Greek NSRF; and the National Priorities Research Program by Qatar National Research Fund; and the Russian Scientific Fund, grant N 14-12-00110.

References

[1] ATLAS Collaboration, "Observation of a new particle in the search for the Standard Model Higgs boson with the ATLAS detector at the LHC", *Phys. Lett. B* **716** (2012) 1, doi:10.1016/j.physletb.2012.08.020, arXiv:1207.7214.

[2] CMS Collaboration, "Observation of a new boson at a mass of 125 GeV with the CMS experiment at the LHC", *Phys. Lett. B* **716** (2012) 30, doi:10.1016/j.physletb.2012.08.021, arXiv:1207.7235.

[3] CMS Collaboration, "Observation of a new boson with mass near 125 GeV in pp collisions at $\sqrt{s}$ = 7 and 8 TeV", *JHEP* **06** (2013) 081, doi:10.1007/JHEP06(2013)081, arXiv:1303.4571.

[4] G. C. Branco et al., "Theory and phenomenology of two-Higgs-doublet models", *Phys. Rept.* **516** (2012) 1, doi:10.1016/j.physrep.2012.02.002, arXiv:1106.0034.

[5] A. Denner, S. Heinemeyer, I. Puljak, D. Rebuzzi, and M. Spira, "Standard Model Higgs-Boson Branching Ratios with Uncertainties", *Eur. Phys. J. C* **71** (2011) 1753, doi:10.1140/epjc/s10052-011-1753-8, arXiv:1107.5909.

[6] CMS Collaboration, "Evidence for the 125 GeV Higgs boson decaying to a pair of τ leptons", *JHEP* **05** (2014) 104, doi:10.1007/JHEP05(2014)104, arXiv:1401.5041.

[7] S. Weinberg, "A Model of Leptons", *Phys. Rev. Lett.* **19** (1967) 1264, doi:10.1103/PhysRevLett.19.1264.

[8] T. Plehn and D. L. Rainwater, "Higgs decays to muons in weak boson fusion", *Phys. Lett. B* **520** (2001) 108, doi:10.1016/S0370-2693(01)01157-1, arXiv:hep-ph/0107180.

[9] T. Han and B. McElrath, "$h \to \mu^+\mu^-$ via gluon fusion at the LHC", *Phys. Lett. B* **528** (2002) 81, doi:10.1016/S0370-2693(02)01208-X, arXiv:hep-ph/0201023.

[10] N. Vignaroli, "Searching for a dilaton decaying to muon pairs at the LHC", *Phys. Rev. D* **80** (2009) 095023, doi:10.1103/PhysRevD.80.095023, arXiv:0906.4078.

[11] A. Dery, A. Efrati, Y. Hochberg, and Y. Nir, "What if BR($h \to \mu\mu$) / BR($h \to \tau\tau$) $\neq m_\mu^2/m_\tau^2$?", *JHEP* **05** (2013) 039, doi:10.1007/JHEP05(2013)039, arXiv:1302.3229.

[12] ATLAS Collaboration, "Search for the Standard Model Higgs boson decay to $\mu^+\mu^-$ with the ATLAS detector", *Phys. Lett. B* **738** (2014) 68, doi:10.1016/j.physletb.2014.09.008, arXiv:1406.7663.

[13] ATLAS Collaboration, "Search for the neutral Higgs bosons of the minimal supersymmetric standard model in pp collisions at $\sqrt{s} = 7$ TeV with the ATLAS detector", *JHEP* **02** (2013) 095, doi:10.1007/JHEP02(2013)095, arXiv:1211.6956.

[14] D. de Florian and M. Grazzini, "Higgs production at the LHC: updated cross sections at $\sqrt{s} = 8$ TeV", *Phys. Lett. B* **718** (2012) 117, doi:10.1016/j.physletb.2012.10.019, arXiv:1206.4133.

[15] LHC Higgs Cross Section Working Group, "Handbook of LHC Higgs Cross Sections: 1. Inclusive Observables", (2011). arXiv:1101.0593.

[16] LHC Higgs Cross Section Working Group, "Handbook of LHC Higgs Cross Sections: 2. Differential Distributions", (2012). arXiv:1201.3084.

[17] LHC Higgs Cross Section Working Group, "Handbook of LHC Higgs Cross Sections: 3. Higgs Properties", (2013). arXiv:1307.1347.

[18] CMS Collaboration, "Constraints on the Higgs boson width from off-shell production and decay to Z-boson pairs", *Phys. Lett. B* **736** (2014) 64, doi:10.1016/j.physletb.2014.06.077, arXiv:1405.3455.

[19] CMS Collaboration, "The CMS experiment at the CERN LHC", *JINST* **3** (2008) S08004, doi:10.1088/1748-0221/3/08/S08004.

[20] CMS Collaboration, "Particle–Flow Event Reconstruction in CMS and Performance for Jets, Taus, and $E_{\mathrm{T}}^{\mathrm{miss}}$", CMS Physics Analysis Summary CMS-PAS-PFT-09-001, 2009.

[21] CMS Collaboration, "Commissioning of the Particle-flow Event Reconstruction with the first LHC collisions recorded in the CMS detector", CMS Physics Analysis Summary CMS-PAS-PFT-10-001, 2010.

[22] M. Cacciari, G. P. Salam, and G. Soyez, "The anti-k_t jet clustering algorithm", *JHEP* **04** (2008) 063, doi:10.1088/1126-6708/2008/04/063, arXiv:0802.1189.

[23] M. Cacciari, G. P. Salam, and G. Soyez, "FastJet user manual", *Eur. Phys. J. C* **72** (2012) 1896, doi:10.1140/epjc/s10052-012-1896-2, arXiv:1111.6097.

[24] CMS Collaboration, "Determination of Jet Energy Calibration and Transverse Momentum Resolution in CMS", *JINST* **6** (2011) P11002, doi:10.1088/1748-0221/6/11/P11002, arXiv:1107.4277.

[25] CMS Collaboration, "Jet Performance in pp Collisions at 7 TeV", CMS Physics Analysis Summary CMS-PAS-JME-10-003, 2010.

[26] CMS Collaboration, "Performance of CMS muon reconstruction in pp collision events at $\sqrt{s} = 7$ TeV", *J. Instrum.* **7** (2012) P10002, doi:10.1088/1748-0221/7/10/P10002.

[27] CMS Collaboration, "Energy calibration and resolution of the CMS electromagnetic calorimeter in pp collisions at $\sqrt{s} = 7$ TeV", *JINST* **8** (2013) P09009, doi:10.1088/1748-0221/8/09/P09009, arXiv:1306.2016.

[28] CMS Collaboration, "Pileup Jet Identification", CMS Physics Analysis Summary CMS-PAS-JME-13-005, 2013.

[29] S. Alioli, P. Nason, C. Oleari, and E. Re, "A general framework for implementing NLO calculations in shower Monte Carlo programs: the POWHEG BOX", *JHEP* **06** (2010) 043, doi:10.1007/JHEP06(2010)043, arXiv:1002.2581.

[30] S. Alioli, P. Nason, C. Oleari, and E. Re, "NLO Higgs boson production via gluon fusion matched with shower in POWHEG", *JHEP* **04** (2009) 002, doi:10.1088/1126-6708/2009/04/002, arXiv:0812.0578.

[31] P. Nason and C. Oleari, "NLO Higgs boson production via vector-boson fusion matched with shower in POWHEG", *JHEP* **02** (2010) 037, doi:10.1007/JHEP02(2010)037, arXiv:0911.5299.

[32] T. Sjöstrand, S. Mrenna, and P. Z. Skands, "PYTHIA 6.4 physics and manual", *JHEP* **05** (2006) 026, doi:10.1088/1126-6708/2006/05/026, arXiv:hep-ph/0603175.

[33] M. Bähr et al., "Herwig++ physics and manual", *Eur. Phys. J. C* **58** (2008) 639, doi:10.1140/epjc/s10052-008-0798-9, arXiv:0803.0883.

[34] GEANT4 Collaboration, "GEANT4—a simulation toolkit", *Nucl. Instrum. Meth. A* **506** (2003) 250, doi:10.1016/S0168-9002(03)01368-8.

[35] J. Alwall et al., "The automated computation of tree-level and next-to-leading order differential cross sections, and their matching to parton shower simulations", *JHEP* **07** (2014) 079, doi:10.1007/JHEP07(2014)079, arXiv:1405.0301.

[36] ATLAS and CMS Collaborations, and LHC Higgs Combination Group, "Procedure for the LHC Higgs boson search combination in summer 2011", CMS Note CMS-NOTE-2011/005 ATL-PHYS-PUB-2011-011, 2011.

[37] S. Alekhin et al., "The PDF4LHC Working Group Interim Report", (2011). arXiv:1101.0536.

[38] M. Botje et al., "The PDF4LHC Working Group Interim Recommendations", (2011). arXiv:1101.0538.

[39] H.-L. Lai et al., "New parton distributions for collider physics", *Phys. Rev. D* **82** (2010) 074024, doi:10.1103/PhysRevD.82.074024, arXiv:1007.2241.

[40] A. D. Martin, W. J. Stirling, R. S. Thorne, and G. Watt, "Parton distributions for the LHC", *Eur. Phys. J. C* **63** (2009) 189, doi:10.1140/epjc/s10052-009-1072-5, arXiv:0901.0002.

[41] NNPDF Collaboration, "A first unbiased global NLO determination of parton distributions and their uncertainties", *Nucl. Phys. B* **838** (2010) 136, doi:10.1016/j.nuclphysb.2010.05.008, arXiv:1002.4407.

[42] M. R. Whalley, D. Bourilkov, and R. C. Group, "The Les Houches accord PDFs (LHAPDF) and LHAGLUE", (2005). arXiv:hep-ph/0508110.

[43] R. Field, "The underlying event in hadronic collisions", *Ann. Rev. Nucl. Part. Sci.* **62** (2012) 453, doi:10.1146/annurev-nucl-102711-095030.

[44] P. Z. Skands, "Tuning Monte Carlo generators: The Perugia tunes", *Phys. Rev. D* **82** (2010) 074018, doi:10.1103/PhysRevD.82.074018, arXiv:1005.3457.

[45] A. Buckley et al., "Systematic event generator tuning for the LHC", *Eur. Phys. J. C* **65** (2010) 331, doi:10.1140/epjc/s10052-009-1196-7, arXiv:0907.2973.

[46] CMS Collaboration, "Absolute Calibration of the Luminosity Measurement at CMS: Winter 2012 Update", CMS Physics Analysis Summary CMS-PAS-SMP-12-008, 2012.

[47] CMS Collaboration, "CMS Luminosity Based on Pixel Cluster Counting - Summer 2013 Update", CMS Physics Analysis Summary CMS-PAS-LUM-13-001, 2013.

[48] A. L. Read, "Presentation of search results: the CLs technique", *J. Phys. G* **28** (2002) 2693, doi:10.1088/0954-3899/28/10/313.

[49] T. Junk, "Confidence level computation for combining searches with small statistics", *Nucl. Instrum. Meth. A* **434** (1999) 435, doi:10.1016/S0168-9002(99)00498-2, arXiv:hep-ex/9902006.

[50] CMS Collaboration, "Combined results of searches for the standard model Higgs boson", *Phys. Lett. B* **710** (2012) 26, doi:10.1016/j.physletb.2012.02.064.

[51] G. Cowan, K. Cranmer, E. Gross, and O. Vitells, "Asymptotic formulae for likelihood-based tests of new physics", *Eur. Phys. J. C* **71** (2011) 1554, doi:10.1140/epjc/s10052-011-1554-0.

[52] CMS Collaboration, "Jet Plus Tracks Algorithm for Calorimeter Jet Energy Corrections in CMS", CMS Physics Analysis Summary CMS-PAS-JME-09-002, 2009.

[53] CMS Collaboration, "Measurement of the properties of a Higgs boson in the four-lepton final state", *Phys. Rev. D* **89** (2013) 092007, doi:10.1103/PhysRevD.89.092007.

[54] CMS Collaboration, "Electron performance with 19.6 fb^{-1} of data collected at $\sqrt{s} = 8$ TeV with the CMS detector.", CMS Detector Performance Summary CMS-DP-2013-003, 2013.

[55] D. L. Rainwater, R. Szalapski, and D. Zeppenfeld, "Probing color singlet exchange in Z + two jet events at the CERN LHC", *Phys. Rev. D* **54** (1996) 6680, doi:10.1103/PhysRevD.54.6680, arXiv:hep-ph/9605444.

[56] CMS Collaboration, "Observation of the diphoton decay of the Higgs boson and measurement of its properties", *Eur. Phys. J. C* **74** (2014) 3076, doi:10.1140/epjc/s10052-014-3076-z, arXiv:1407.0558.

A The CMS Collaboration

Yerevan Physics Institute, Yerevan, Armenia
V. Khachatryan, A.M. Sirunyan, A. Tumasyan

Institut für Hochenergiephysik der OeAW, Wien, Austria
W. Adam, T. Bergauer, M. Dragicevic, J. Erö, C. Fabjan[1], M. Friedl, R. Frühwirth[1], V.M. Ghete, C. Hartl, N. Hörmann, J. Hrubec, M. Jeitler[1], W. Kiesenhofer, V. Knünz, M. Krammer[1], I. Krätschmer, D. Liko, I. Mikulec, D. Rabady[2], B. Rahbaran, H. Rohringer, R. Schöfbeck, J. Strauss, A. Taurok, W. Treberer-Treberspurg, W. Waltenberger, C.-E. Wulz[1]

National Centre for Particle and High Energy Physics, Minsk, Belarus
V. Mossolov, N. Shumeiko, J. Suarez Gonzalez

Universiteit Antwerpen, Antwerpen, Belgium
S. Alderweireldt, M. Bansal, S. Bansal, T. Cornelis, E.A. De Wolf, X. Janssen, A. Knutsson, S. Luyckx, S. Ochesanu, R. Rougny, M. Van De Klundert, H. Van Haevermaet, P. Van Mechelen, N. Van Remortel, A. Van Spilbeeck

Vrije Universiteit Brussel, Brussel, Belgium
F. Blekman, S. Blyweert, J. D'Hondt, N. Daci, N. Heracleous, J. Keaveney, S. Lowette, M. Maes, A. Olbrechts, Q. Python, D. Strom, S. Tavernier, W. Van Doninck, P. Van Mulders, G.P. Van Onsem, I. Villella

Université Libre de Bruxelles, Bruxelles, Belgium
C. Caillol, B. Clerbaux, G. De Lentdecker, D. Dobur, L. Favart, A.P.R. Gay, A. Grebenyuk, A. Léonard, A. Mohammadi, L. Perniè[2], T. Reis, T. Seva, L. Thomas, C. Vander Velde, P. Vanlaer, J. Wang, F. Zenoni

Ghent University, Ghent, Belgium
V. Adler, K. Beernaert, L. Benucci, A. Cimmino, S. Costantini, S. Crucy, S. Dildick, A. Fagot, G. Garcia, J. Mccartin, A.A. Ocampo Rios, D. Ryckbosch, S. Salva Diblen, M. Sigamani, N. Strobbe, F. Thyssen, M. Tytgat, E. Yazgan, N. Zaganidis

Université Catholique de Louvain, Louvain-la-Neuve, Belgium
S. Basegmez, C. Beluffi[3], G. Bruno, R. Castello, A. Caudron, L. Ceard, G.G. Da Silveira, C. Delaere, T. du Pree, D. Favart, L. Forthomme, A. Giammanco[4], J. Hollar, A. Jafari, P. Jez, M. Komm, V. Lemaitre, C. Nuttens, D. Pagano, L. Perrini, A. Pin, K. Piotrzkowski, A. Popov[5], L. Quertenmont, M. Selvaggi, M. Vidal Marono, J.M. Vizan Garcia

Université de Mons, Mons, Belgium
N. Beliy, T. Caebergs, E. Daubie, G.H. Hammad

Centro Brasileiro de Pesquisas Fisicas, Rio de Janeiro, Brazil
W.L. Aldá Júnior, G.A. Alves, L. Brito, M. Correa Martins Junior, T. Dos Reis Martins, C. Mora Herrera, M.E. Pol

Universidade do Estado do Rio de Janeiro, Rio de Janeiro, Brazil
W. Carvalho, J. Chinellato[6], A. Custódio, E.M. Da Costa, D. De Jesus Damiao, C. De Oliveira Martins, S. Fonseca De Souza, H. Malbouisson, D. Matos Figueiredo, L. Mundim, H. Nogima, W.L. Prado Da Silva, J. Santaolalla, A. Santoro, A. Sznajder, E.J. Tonelli Manganote[6], A. Vilela Pereira

Universidade Estadual Paulista [a], Universidade Federal do ABC [b], São Paulo, Brazil
C.A. Bernardes[b], S. Dogra[a], T.R. Fernandez Perez Tomei[a], E.M. Gregores[b], P.G. Mercadante[b], S.F. Novaes[a], Sandra S. Padula[a]

Institute for Nuclear Research and Nuclear Energy, Sofia, Bulgaria
A. Aleksandrov, V. Genchev[2], P. Iaydjiev, A. Marinov, S. Piperov, M. Rodozov, S. Stoykova, G. Sultanov, V. Tcholakov, M. Vutova

University of Sofia, Sofia, Bulgaria
A. Dimitrov, I. Glushkov, R. Hadjiiska, V. Kozhuharov, L. Litov, B. Pavlov, P. Petkov

Institute of High Energy Physics, Beijing, China
J.G. Bian, G.M. Chen, H.S. Chen, M. Chen, R. Du, C.H. Jiang, R. Plestina[7], F. Romeo, J. Tao, Z. Wang

State Key Laboratory of Nuclear Physics and Technology, Peking University, Beijing, China
C. Asawatangtrakuldee, Y. Ban, Q. Li, S. Liu, Y. Mao, S.J. Qian, D. Wang, W. Zou

Universidad de Los Andes, Bogota, Colombia
C. Avila, L.F. Chaparro Sierra, C. Florez, J.P. Gomez, B. Gomez Moreno, J.C. Sanabria

University of Split, Faculty of Electrical Engineering, Mechanical Engineering and Naval Architecture, Split, Croatia
N. Godinovic, D. Lelas, D. Polic, I. Puljak

University of Split, Faculty of Science, Split, Croatia
Z. Antunovic, M. Kovac

Institute Rudjer Boskovic, Zagreb, Croatia
V. Brigljevic, K. Kadija, J. Luetic, D. Mekterovic, L. Sudic

University of Cyprus, Nicosia, Cyprus
A. Attikis, G. Mavromanolakis, J. Mousa, C. Nicolaou, F. Ptochos, P.A. Razis

Charles University, Prague, Czech Republic
M. Bodlak, M. Finger, M. Finger Jr.[8]

Academy of Scientific Research and Technology of the Arab Republic of Egypt, Egyptian Network of High Energy Physics, Cairo, Egypt
Y. Assran[9], A. Ellithi Kamel[10], M.A. Mahmoud[11], A. Radi[12,13]

National Institute of Chemical Physics and Biophysics, Tallinn, Estonia
M. Kadastik, M. Murumaa, M. Raidal, A. Tiko

Department of Physics, University of Helsinki, Helsinki, Finland
P. Eerola, G. Fedi, M. Voutilainen

Helsinki Institute of Physics, Helsinki, Finland
J. Härkönen, V. Karimäki, R. Kinnunen, M.J. Kortelainen, T. Lampén, K. Lassila-Perini, S. Lehti, T. Lindén, P. Luukka, T. Mäenpää, T. Peltola, E. Tuominen, J. Tuominiemi, E. Tuovinen, L. Wendland

Lappeenranta University of Technology, Lappeenranta, Finland
J. Talvitie, T. Tuuva

DSM/IRFU, CEA/Saclay, Gif-sur-Yvette, France
M. Besancon, F. Couderc, M. Dejardin, D. Denegri, B. Fabbro, J.L. Faure, C. Favaro, F. Ferri,

S. Ganjour, A. Givernaud, P. Gras, G. Hamel de Monchenault, P. Jarry, E. Locci, J. Malcles, J. Rander, A. Rosowsky, M. Titov

Laboratoire Leprince-Ringuet, Ecole Polytechnique, IN2P3-CNRS, Palaiseau, France
S. Baffioni, F. Beaudette, P. Busson, C. Charlot, T. Dahms, M. Dalchenko, L. Dobrzynski, N. Filipovic, A. Florent, R. Granier de Cassagnac, L. Mastrolorenzo, P. Miné, C. Mironov, I.N. Naranjo, M. Nguyen, C. Ochando, P. Paganini, S. Regnard, R. Salerno, J.B. Sauvan, Y. Sirois, C. Veelken, Y. Yilmaz, A. Zabi

Institut Pluridisciplinaire Hubert Curien, Université de Strasbourg, Université de Haute Alsace Mulhouse, CNRS/IN2P3, Strasbourg, France
J.-L. Agram[14], J. Andrea, A. Aubin, D. Bloch, J.-M. Brom, E.C. Chabert, C. Collard, E. Conte[14], J.-C. Fontaine[14], D. Gelé, U. Goerlach, C. Goetzmann, A.-C. Le Bihan, P. Van Hove

Centre de Calcul de l'Institut National de Physique Nucleaire et de Physique des Particules, CNRS/IN2P3, Villeurbanne, France
S. Gadrat

Université de Lyon, Université Claude Bernard Lyon 1, CNRS-IN2P3, Institut de Physique Nucléaire de Lyon, Villeurbanne, France
S. Beauceron, N. Beaupere, G. Boudoul[2], E. Bouvier, S. Brochet, C.A. Carrillo Montoya, J. Chasserat, R. Chierici, D. Contardo[2], P. Depasse, H. El Mamouni, J. Fan, J. Fay, S. Gascon, M. Gouzevitch, B. Ille, T. Kurca, M. Lethuillier, L. Mirabito, S. Perries, J.D. Ruiz Alvarez, D. Sabes, L. Sgandurra, V. Sordini, M. Vander Donckt, P. Verdier, S. Viret, H. Xiao

Institute of High Energy Physics and Informatization, Tbilisi State University, Tbilisi, Georgia
Z. Tsamalaidze[8]

RWTH Aachen University, I. Physikalisches Institut, Aachen, Germany
C. Autermann, S. Beranek, M. Bontenackels, M. Edelhoff, L. Feld, O. Hindrichs, K. Klein, A. Ostapchuk, A. Perieanu, F. Raupach, J. Sammet, S. Schael, H. Weber, B. Wittmer, V. Zhukov[5]

RWTH Aachen University, III. Physikalisches Institut A, Aachen, Germany
M. Ata, M. Brodski, E. Dietz-Laursonn, D. Duchardt, M. Erdmann, R. Fischer, A. Güth, T. Hebbeker, C. Heidemann, K. Hoepfner, D. Klingebiel, S. Knutzen, P. Kreuzer, M. Merschmeyer, A. Meyer, P. Millet, M. Olschewski, K. Padeken, P. Papacz, H. Reithler, S.A. Schmitz, L. Sonnenschein, D. Teyssier, S. Thüer, M. Weber

RWTH Aachen University, III. Physikalisches Institut B, Aachen, Germany
V. Cherepanov, Y. Erdogan, G. Flügge, H. Geenen, M. Geisler, W. Haj Ahmad, A. Heister, F. Hoehle, B. Kargoll, T. Kress, Y. Kuessel, A. Künsken, J. Lingemann[2], A. Nowack, I.M. Nugent, L. Perchalla, O. Pooth, A. Stahl

Deutsches Elektronen-Synchrotron, Hamburg, Germany
I. Asin, N. Bartosik, J. Behr, W. Behrenhoff, U. Behrens, A.J. Bell, M. Bergholz[15], A. Bethani, K. Borras, A. Burgmeier, A. Cakir, L. Calligaris, A. Campbell, S. Choudhury, F. Costanza, C. Diez Pardos, S. Dooling, T. Dorland, G. Eckerlin, D. Eckstein, T. Eichhorn, G. Flucke, J. Garay Garcia, A. Geiser, P. Gunnellini, J. Hauk, M. Hempel[15], D. Horton, H. Jung, A. Kalogeropoulos, M. Kasemann, P. Katsas, J. Kieseler, C. Kleinwort, D. Krücker, W. Lange, J. Leonard, K. Lipka, A. Lobanov, W. Lohmann[15], B. Lutz, R. Mankel, I. Marfin[15], I.-A. Melzer-Pellmann, A.B. Meyer, G. Mittag, J. Mnich, A. Mussgiller, S. Naumann-Emme, A. Nayak, O. Novgorodova, E. Ntomari, H. Perrey, D. Pitzl, R. Placakyte, A. Raspereza, P.M. Ribeiro Cipriano, B. Roland, E. Ron, M.Ö. Sahin, J. Salfeld-Nebgen, P. Saxena, R. Schmidt[15],

T. Schoerner-Sadenius, M. Schröder, C. Seitz, S. Spannagel, A.D.R. Vargas Trevino, R. Walsh, C. Wissing

University of Hamburg, Hamburg, Germany
M. Aldaya Martin, V. Blobel, M. Centis Vignali, A.R. Draeger, J. Erfle, E. Garutti, K. Goebel, M. Görner, J. Haller, M. Hoffmann, R.S. Höing, H. Kirschenmann, R. Klanner, R. Kogler, J. Lange, T. Lapsien, T. Lenz, I. Marchesini, J. Ott, T. Peiffer, N. Pietsch, J. Poehlsen, T. Poehlsen, D. Rathjens, C. Sander, H. Schettler, P. Schleper, E. Schlieckau, A. Schmidt, M. Seidel, V. Sola, H. Stadie, G. Steinbrück, D. Troendle, E. Usai, L. Vanelderen, A. Vanhoefer

Institut für Experimentelle Kernphysik, Karlsruhe, Germany
C. Barth, C. Baus, J. Berger, C. Böser, E. Butz, T. Chwalek, W. De Boer, A. Descroix, A. Dierlamm, M. Feindt, F. Frensch, M. Giffels, F. Hartmann[2], T. Hauth[2], U. Husemann, I. Katkov[5], A. Kornmayer[2], E. Kuznetsova, P. Lobelle Pardo, M.U. Mozer, Th. Müller, A. Nürnberg, G. Quast, K. Rabbertz, F. Ratnikov, S. Röcker, H.J. Simonis, F.M. Stober, R. Ulrich, J. Wagner-Kuhr, S. Wayand, T. Weiler, R. Wolf

Institute of Nuclear and Particle Physics (INPP), NCSR Demokritos, Aghia Paraskevi, Greece
G. Anagnostou, G. Daskalakis, T. Geralis, V.A. Giakoumopoulou, A. Kyriakis, D. Loukas, A. Markou, C. Markou, A. Psallidas, I. Topsis-Giotis

University of Athens, Athens, Greece
A. Agapitos, S. Kesisoglou, A. Panagiotou, N. Saoulidou, E. Stiliaris

University of Ioánnina, Ioánnina, Greece
X. Aslanoglou, I. Evangelou, G. Flouris, C. Foudas, P. Kokkas, N. Manthos, I. Papadopoulos, E. Paradas

Wigner Research Centre for Physics, Budapest, Hungary
G. Bencze, C. Hajdu, P. Hidas, D. Horvath[16], F. Sikler, V. Veszpremi, G. Vesztergombi[17], A.J. Zsigmond

Institute of Nuclear Research ATOMKI, Debrecen, Hungary
N. Beni, S. Czellar, J. Karancsi[18], J. Molnar, J. Palinkas, Z. Szillasi

University of Debrecen, Debrecen, Hungary
P. Raics, Z.L. Trocsanyi, B. Ujvari

National Institute of Science Education and Research, Bhubaneswar, India
S.K. Swain

Panjab University, Chandigarh, India
S.B. Beri, V. Bhatnagar, R. Gupta, U.Bhawandeep, A.K. Kalsi, M. Kaur, R. Kumar, M. Mittal, N. Nishu, J.B. Singh

University of Delhi, Delhi, India
Ashok Kumar, Arun Kumar, S. Ahuja, A. Bhardwaj, B.C. Choudhary, A. Kumar, S. Malhotra, M. Naimuddin, K. Ranjan, V. Sharma

Saha Institute of Nuclear Physics, Kolkata, India
S. Banerjee, S. Bhattacharya, K. Chatterjee, S. Dutta, B. Gomber, Sa. Jain, Sh. Jain, R. Khurana, A. Modak, S. Mukherjee, D. Roy, S. Sarkar, M. Sharan

Bhabha Atomic Research Centre, Mumbai, India
A. Abdulsalam, D. Dutta, S. Kailas, V. Kumar, A.K. Mohanty[2], L.M. Pant, P. Shukla, A. Topkar

Tata Institute of Fundamental Research, Mumbai, India
T. Aziz, S. Banerjee, S. Bhowmik[19], R.M. Chatterjee, R.K. Dewanjee, S. Dugad, S. Ganguly, S. Ghosh, M. Guchait, A. Gurtu[20], G. Kole, S. Kumar, M. Maity[19], G. Majumder, K. Mazumdar, G.B. Mohanty, B. Parida, K. Sudhakar, N. Wickramage[21]

Institute for Research in Fundamental Sciences (IPM), Tehran, Iran
H. Bakhshiansohi, H. Behnamian, S.M. Etesami[22], A. Fahim[23], R. Goldouzian, M. Khakzad, M. Mohammadi Najafabadi, M. Naseri, S. Paktinat Mehdiabadi, F. Rezaei Hosseinabadi, B. Safarzadeh[24], M. Zeinali

University College Dublin, Dublin, Ireland
M. Felcini, M. Grunewald

INFN Sezione di Bari [a], Università di Bari [b], Politecnico di Bari [c], Bari, Italy
M. Abbrescia[a,b], L. Barbone[a,b], C. Calabria[a,b], S.S. Chhibra[a,b], A. Colaleo[a], D. Creanza[a,c], N. De Filippis[a,c], M. De Palma[a,b], L. Fiore[a], G. Iaselli[a,c], G. Maggi[a,c], M. Maggi[a], S. My[a,c], S. Nuzzo[a,b], A. Pompili[a,b], G. Pugliese[a,c], R. Radogna[a,b,2], G. Selvaggi[a,b], L. Silvestris[a,2], R. Venditti[a,b], G. Zito[a]

INFN Sezione di Bologna [a], Università di Bologna [b], Bologna, Italy
G. Abbiendi[a], A.C. Benvenuti[a], D. Bonacorsi[a,b], S. Braibant-Giacomelli[a,b], L. Brigliadori[a,b], R. Campanini[a,b], P. Capiluppi[a,b], A. Castro[a,b], F.R. Cavallo[a], G. Codispoti[a,b], M. Cuffiani[a,b], G.M. Dallavalle[a], F. Fabbri[a], A. Fanfani[a,b], D. Fasanella[a,b], P. Giacomelli[a], C. Grandi[a], L. Guiducci[a,b], S. Marcellini[a], G. Masetti[a], A. Montanari[a], F.L. Navarria[a,b], A. Perrotta[a], F. Primavera[a,b], A.M. Rossi[a,b], T. Rovelli[a,b], G.P. Siroli[a,b], N. Tosi[a,b], R. Travaglini[a,b]

INFN Sezione di Catania [a], Università di Catania [b], CSFNSM [c], Catania, Italy
S. Albergo[a,b], G. Cappello[a], M. Chiorboli[a,b], S. Costa[a,b], F. Giordano[a,2], R. Potenza[a,b], A. Tricomi[a,b], C. Tuve[a,b]

INFN Sezione di Firenze [a], Università di Firenze [b], Firenze, Italy
G. Barbagli[a], V. Ciulli[a,b], C. Civinini[a], R. D'Alessandro[a,b], E. Focardi[a,b], E. Gallo[a], S. Gonzi[a,b], V. Gori[a,b,2], P. Lenzi[a,b], M. Meschini[a], S. Paoletti[a], G. Sguazzoni[a], A. Tropiano[a,b]

INFN Laboratori Nazionali di Frascati, Frascati, Italy
L. Benussi, S. Bianco, F. Fabbri, D. Piccolo

INFN Sezione di Genova [a], Università di Genova [b], Genova, Italy
R. Ferretti[a,b], F. Ferro[a], M. Lo Vetere[a,b], E. Robutti[a], S. Tosi[a,b]

INFN Sezione di Milano-Bicocca [a], Università di Milano-Bicocca [b], Milano, Italy
M.E. Dinardo[a,b], S. Fiorendi[a,b], S. Gennai[a,2], R. Gerosa[a,b,2], A. Ghezzi[a,b], P. Govoni[a,b], M.T. Lucchini[a,b,2], S. Malvezzi[a], R.A. Manzoni[a,b], A. Martelli[a,b], B. Marzocchi[a,b,2], D. Menasce[a], L. Moroni[a], M. Paganoni[a,b], D. Pedrini[a], S. Ragazzi[a,b], N. Redaelli[a], T. Tabarelli de Fatis[a,b]

INFN Sezione di Napoli [a], Università di Napoli 'Federico II' [b], Università della Basilicata (Potenza) [c], Università G. Marconi (Roma) [d], Napoli, Italy
S. Buontempo[a], N. Cavallo[a,c], S. Di Guida[a,d,2], F. Fabozzi[a,c], A.O.M. Iorio[a,b], L. Lista[a], S. Meola[a,d,2], M. Merola[a], P. Paolucci[a,2]

INFN Sezione di Padova [a], Università di Padova [b], Università di Trento (Trento) [c], Padova, Italy
P. Azzi[a], N. Bacchetta[a], D. Bisello[a,b], A. Branca[a,b], R. Carlin[a,b], P. Checchia[a], M. Dall'Osso[a,b], T. Dorigo[a], U. Dosselli[a], M. Galanti[a,b], F. Gasparini[a,b], U. Gasparini[a,b], P. Giubilato[a,b], A. Gozzelino[a], K. Kanishchev[a,c], S. Lacaprara[a], M. Margoni[a,b], A.T. Meneguzzo[a,b], J. Pazzini[a,b],

N. Pozzobon[a,b], P. Ronchese[a,b], F. Simonetto[a,b], E. Torassa[a], M. Tosi[a,b], P. Zotto[a,b], A. Zucchetta[a,b], G. Zumerle[a,b]

INFN Sezione di Pavia [a], Università di Pavia [b], Pavia, Italy
M. Gabusi[a,b], S.P. Ratti[a,b], V. Re[a], C. Riccardi[a,b], P. Salvini[a], P. Vitulo[a,b]

INFN Sezione di Perugia [a], Università di Perugia [b], Perugia, Italy
M. Biasini[a,b], G.M. Bilei[a], D. Ciangottini[a,b], L. Fanò[a,b], P. Lariccia[a,b], G. Mantovani[a,b], M. Menichelli[a], A. Saha[a], A. Santocchia[a,b], A. Spiezia[a,b,2]

INFN Sezione di Pisa [a], Università di Pisa [b], Scuola Normale Superiore di Pisa [c], Pisa, Italy
K. Androsov[a,25], P. Azzurri[a], G. Bagliesi[a], J. Bernardini[a], T. Boccali[a], G. Broccolo[a,c], R. Castaldi[a], M.A. Ciocci[a,25], R. Dell'Orso[a], S. Donato[a,c], F. Fiori[a,c], L. Foà[a,c], A. Giassi[a], M.T. Grippo[a,25], F. Ligabue[a,c], T. Lomtadze[a], L. Martini[a,b], A. Messineo[a,b], C.S. Moon[a,26], F. Palla[a,2], A. Rizzi[a,b], A. Savoy-Navarro[a,27], A.T. Serban[a], P. Spagnolo[a], P. Squillacioti[a,25], R. Tenchini[a], G. Tonelli[a,b], A. Venturi[a], P.G. Verdini[a], C. Vernieri[a,c,2]

INFN Sezione di Roma [a], Università di Roma [b], Roma, Italy
L. Barone[a,b], F. Cavallari[a], G. D'imperio[a,b], D. Del Re[a,b], M. Diemoz[a], M. Grassi[a,b], C. Jorda[a], E. Longo[a,b], F. Margaroli[a,b], P. Meridiani[a], F. Micheli[a,b,2], S. Nourbakhsh[a,b], G. Organtini[a,b], R. Paramatti[a], S. Rahatlou[a,b], C. Rovelli[a], F. Santanastasio[a,b], L. Soffi[a,b,2], P. Traczyk[a,b]

INFN Sezione di Torino [a], Università di Torino [b], Università del Piemonte Orientale (Novara) [c], Torino, Italy
N. Amapane[a,b], R. Arcidiacono[a,c], S. Argiro[a,b,2], M. Arneodo[a,c], R. Bellan[a,b], C. Biino[a], N. Cartiglia[a], S. Casasso[a,b,2], M. Costa[a,b], A. Degano[a,b], N. Demaria[a], L. Finco[a,b], C. Mariotti[a], S. Maselli[a], E. Migliore[a,b], V. Monaco[a,b], M. Musich[a], M.M. Obertino[a,c,2], G. Ortona[a,b], L. Pacher[a,b], N. Pastrone[a], M. Pelliccioni[a], G.L. Pinna Angioni[a,b], A. Potenza[a,b], A. Romero[a,b], M. Ruspa[a,c], R. Sacchi[a,b], A. Solano[a,b], A. Staiano[a], U. Tamponi[a]

INFN Sezione di Trieste [a], Università di Trieste [b], Trieste, Italy
S. Belforte[a], V. Candelise[a,b], M. Casarsa[a], F. Cossutti[a], G. Della Ricca[a,b], B. Gobbo[a], C. La Licata[a,b], M. Marone[a,b], A. Schizzi[a,b], T. Umer[a,b], A. Zanetti[a]

Kangwon National University, Chunchon, Korea
S. Chang, A. Kropivnitskaya, S.K. Nam

Kyungpook National University, Daegu, Korea
D.H. Kim, G.N. Kim, M.S. Kim, D.J. Kong, S. Lee, Y.D. Oh, H. Park, A. Sakharov, D.C. Son

Chonbuk National University, Jeonju, Korea
T.J. Kim

Chonnam National University, Institute for Universe and Elementary Particles, Kwangju, Korea
J.Y. Kim, S. Song

Korea University, Seoul, Korea
S. Choi, D. Gyun, B. Hong, M. Jo, H. Kim, Y. Kim, B. Lee, K.S. Lee, S.K. Park, Y. Roh

University of Seoul, Seoul, Korea
M. Choi, J.H. Kim, I.C. Park, G. Ryu, M.S. Ryu

Sungkyunkwan University, Suwon, Korea
Y. Choi, Y.K. Choi, J. Goh, D. Kim, E. Kwon, J. Lee, H. Seo, I. Yu

Vilnius University, Vilnius, Lithuania
A. Juodagalvis

National Centre for Particle Physics, Universiti Malaya, Kuala Lumpur, Malaysia
J.R. Komaragiri, M.A.B. Md Ali

Centro de Investigacion y de Estudios Avanzados del IPN, Mexico City, Mexico
H. Castilla-Valdez, E. De La Cruz-Burelo, I. Heredia-de La Cruz[28], A. Hernandez-Almada, R. Lopez-Fernandez, A. Sanchez-Hernandez

Universidad Iberoamericana, Mexico City, Mexico
S. Carrillo Moreno, F. Vazquez Valencia

Benemerita Universidad Autonoma de Puebla, Puebla, Mexico
I. Pedraza, H.A. Salazar Ibarguen

Universidad Autónoma de San Luis Potosí, San Luis Potosí, Mexico
E. Casimiro Linares, A. Morelos Pineda

University of Auckland, Auckland, New Zealand
D. Krofcheck

University of Canterbury, Christchurch, New Zealand
P.H. Butler, S. Reucroft

National Centre for Physics, Quaid-I-Azam University, Islamabad, Pakistan
A. Ahmad, M. Ahmad, Q. Hassan, H.R. Hoorani, S. Khalid, W.A. Khan, T. Khurshid, M.A. Shah, M. Shoaib

National Centre for Nuclear Research, Swierk, Poland
H. Bialkowska, M. Bluj, B. Boimska, T. Frueboes, M. Górski, M. Kazana, K. Nawrocki, K. Romanowska-Rybinska, M. Szleper, P. Zalewski

Institute of Experimental Physics, Faculty of Physics, University of Warsaw, Warsaw, Poland
G. Brona, K. Bunkowski, M. Cwiok, W. Dominik, K. Doroba, A. Kalinowski, M. Konecki, J. Krolikowski, M. Misiura, M. Olszewski, W. Wolszczak

Laboratório de Instrumentação e Física Experimental de Partículas, Lisboa, Portugal
P. Bargassa, C. Beirão Da Cruz E Silva, P. Faccioli, P.G. Ferreira Parracho, M. Gallinaro, L. Lloret Iglesias, F. Nguyen, J. Rodrigues Antunes, J. Seixas, J. Varela, P. Vischia

Joint Institute for Nuclear Research, Dubna, Russia
P. Bunin, I. Golutvin, I. Gorbunov, A. Kamenev, V. Karjavin, V. Konoplyanikov, A. Lanev, A. Malakhov, V. Matveev[29], P. Moisenz, V. Palichik, V. Perelygin, M. Savina, S. Shmatov, S. Shulha, N. Skatchkov, V. Smirnov, A. Zarubin

Petersburg Nuclear Physics Institute, Gatchina (St. Petersburg), Russia
V. Golovtsov, Y. Ivanov, V. Kim[30], P. Levchenko, V. Murzin, V. Oreshkin, I. Smirnov, V. Sulimov, L. Uvarov, S. Vavilov, A. Vorobyev, An. Vorobyev

Institute for Nuclear Research, Moscow, Russia
Yu. Andreev, A. Dermenev, S. Gninenko, N. Golubev, M. Kirsanov, N. Krasnikov, A. Pashenkov, D. Tlisov, A. Toropin

Institute for Theoretical and Experimental Physics, Moscow, Russia
V. Epshteyn, V. Gavrilov, N. Lychkovskaya, V. Popov, G. Safronov, S. Semenov, A. Spiridonov, V. Stolin, E. Vlasov, A. Zhokin

P.N. Lebedev Physical Institute, Moscow, Russia
V. Andreev, M. Azarkin, I. Dremin, M. Kirakosyan, A. Leonidov, G. Mesyats, S.V. Rusakov, A. Vinogradov

Skobeltsyn Institute of Nuclear Physics, Lomonosov Moscow State University, Moscow, Russia
A. Belyaev, E. Boos, V. Bunichev, M. Dubinin[31], L. Dudko, A. Ershov, V. Klyukhin, O. Kodolova, I. Lokhtin, S. Obraztsov, M. Perfilov, S. Petrushanko, V. Savrin

State Research Center of Russian Federation, Institute for High Energy Physics, Protvino, Russia
I. Azhgirey, I. Bayshev, S. Bitioukov, V. Kachanov, A. Kalinin, D. Konstantinov, V. Krychkine, V. Petrov, R. Ryutin, A. Sobol, L. Tourtchanovitch, S. Troshin, N. Tyurin, A. Uzunian, A. Volkov

University of Belgrade, Faculty of Physics and Vinca Institute of Nuclear Sciences, Belgrade, Serbia
P. Adzic[32], M. Ekmedzic, J. Milosevic, V. Rekovic

Centro de Investigaciones Energéticas Medioambientales y Tecnológicas (CIEMAT), Madrid, Spain
J. Alcaraz Maestre, C. Battilana, E. Calvo, M. Cerrada, M. Chamizo Llatas, N. Colino, B. De La Cruz, A. Delgado Peris, D. Domínguez Vázquez, A. Escalante Del Valle, C. Fernandez Bedoya, J.P. Fernández Ramos, J. Flix, M.C. Fouz, P. Garcia-Abia, O. Gonzalez Lopez, S. Goy Lopez, J.M. Hernandez, M.I. Josa, E. Navarro De Martino, A. Pérez-Calero Yzquierdo, J. Puerta Pelayo, A. Quintario Olmeda, I. Redondo, L. Romero, M.S. Soares

Universidad Autónoma de Madrid, Madrid, Spain
C. Albajar, J.F. de Trocóniz, M. Missiroli, D. Moran

Universidad de Oviedo, Oviedo, Spain
H. Brun, J. Cuevas, J. Fernandez Menendez, S. Folgueras, I. Gonzalez Caballero

Instituto de Física de Cantabria (IFCA), CSIC-Universidad de Cantabria, Santander, Spain
J.A. Brochero Cifuentes, I.J. Cabrillo, A. Calderon, J. Duarte Campderros, M. Fernandez, G. Gomez, A. Graziano, A. Lopez Virto, J. Marco, R. Marco, C. Martinez Rivero, F. Matorras, F.J. Munoz Sanchez, J. Piedra Gomez, T. Rodrigo, A.Y. Rodríguez-Marrero, A. Ruiz-Jimeno, L. Scodellaro, I. Vila, R. Vilar Cortabitarte

CERN, European Organization for Nuclear Research, Geneva, Switzerland
D. Abbaneo, E. Auffray, G. Auzinger, M. Bachtis, P. Baillon, A.H. Ball, D. Barney, A. Benaglia, J. Bendavid, L. Benhabib, J.F. Benitez, C. Bernet[7], G. Bianchi, P. Bloch, A. Bocci, A. Bonato, O. Bondu, C. Botta, H. Breuker, T. Camporesi, G. Cerminara, S. Colafranceschi[33], M. D'Alfonso, D. d'Enterria, A. Dabrowski, A. David, F. De Guio, A. De Roeck, S. De Visscher, E. Di Marco, M. Dobson, M. Dordevic, N. Dupont-Sagorin, A. Elliott-Peisert, J. Eugster, G. Franzoni, W. Funk, D. Gigi, K. Gill, D. Giordano, M. Girone, F. Glege, R. Guida, S. Gundacker, M. Guthoff, J. Hammer, M. Hansen, P. Harris, J. Hegeman, V. Innocente, P. Janot, K. Kousouris, K. Krajczar, P. Lecoq, C. Lourenço, N. Magini, L. Malgeri, M. Mannelli, J. Marrouche, L. Masetti, F. Meijers, S. Mersi, E. Meschi, F. Moortgat, S. Morovic, M. Mulders, P. Musella, L. Orsini, L. Pape, E. Perez, L. Perrozzi, A. Petrilli, G. Petrucciani, A. Pfeiffer, M. Pierini, M. Pimiä, D. Piparo, M. Plagge, A. Racz, G. Rolandi[34], M. Rovere, H. Sakulin, C. Schäfer, C. Schwick, A. Sharma, P. Siegrist, P. Silva, M. Simon, P. Sphicas[35], D. Spiga, J. Steggemann, B. Stieger, M. Stoye, Y. Takahashi, D. Treille, A. Tsirou, G.I. Veres[17], N. Wardle, H.K. Wöhri, H. Wollny, W.D. Zeuner

Paul Scherrer Institut, Villigen, Switzerland
W. Bertl, K. Deiters, W. Erdmann, R. Horisberger, Q. Ingram, H.C. Kaestli, D. Kotlinski, U. Langenegger, D. Renker, T. Rohe

Institute for Particle Physics, ETH Zurich, Zurich, Switzerland
F. Bachmair, L. Bäni, L. Bianchini, M.A. Buchmann, B. Casal, N. Chanon, G. Dissertori, M. Dittmar, M. Donegà, M. Dünser, P. Eller, C. Grab, D. Hits, J. Hoss, W. Lustermann, B. Mangano, A.C. Marini, P. Martinez Ruiz del Arbol, M. Masciovecchio, D. Meister, N. Mohr, C. Nägeli[36], F. Nessi-Tedaldi, F. Pandolfi, F. Pauss, M. Peruzzi, M. Quittnat, L. Rebane, M. Rossini, A. Starodumov[37], M. Takahashi, K. Theofilatos, R. Wallny, H.A. Weber

Universität Zürich, Zurich, Switzerland
C. Amsler[38], M.F. Canelli, V. Chiochia, A. De Cosa, A. Hinzmann, T. Hreus, B. Kilminster, C. Lange, B. Millan Mejias, J. Ngadiuba, P. Robmann, F.J. Ronga, S. Taroni, M. Verzetti, Y. Yang

National Central University, Chung-Li, Taiwan
M. Cardaci, K.H. Chen, C. Ferro, C.M. Kuo, W. Lin, Y.J. Lu, R. Volpe, S.S. Yu

National Taiwan University (NTU), Taipei, Taiwan
P. Chang, Y.H. Chang, Y.W. Chang, Y. Chao, K.F. Chen, P.H. Chen, C. Dietz, U. Grundler, W.-S. Hou, K.Y. Kao, Y.J. Lei, Y.F. Liu, R.-S. Lu, D. Majumder, E. Petrakou, Y.M. Tzeng, R. Wilken

Chulalongkorn University, Faculty of Science, Department of Physics, Bangkok, Thailand
B. Asavapibhop, G. Singh, N. Srimanobhas, N. Suwonjandee

Cukurova University, Adana, Turkey
A. Adiguzel, M.N. Bakirci[39], S. Cerci[40], C. Dozen, I. Dumanoglu, E. Eskut, S. Girgis, G. Gokbulut, E. Gurpinar, I. Hos, E.E. Kangal, A. Kayis Topaksu, G. Onengut[41], K. Ozdemir, S. Ozturk[39], A. Polatoz, D. Sunar Cerci[40], B. Tali[40], H. Topakli[39], M. Vergili

Middle East Technical University, Physics Department, Ankara, Turkey
I.V. Akin, B. Bilin, S. Bilmis, H. Gamsizkan[42], G. Karapinar[43], K. Ocalan[44], S. Sekmen, U.E. Surat, M. Yalvac, M. Zeyrek

Bogazici University, Istanbul, Turkey
E. Gülmez, B. Isildak[45], M. Kaya[46], O. Kaya[47]

Istanbul Technical University, Istanbul, Turkey
K. Cankocak, F.I. Vardarlı

National Scientific Center, Kharkov Institute of Physics and Technology, Kharkov, Ukraine
L. Levchuk, P. Sorokin

University of Bristol, Bristol, United Kingdom
J.J. Brooke, E. Clement, D. Cussans, H. Flacher, J. Goldstein, M. Grimes, G.P. Heath, H.F. Heath, J. Jacob, L. Kreczko, C. Lucas, Z. Meng, D.M. Newbold[48], S. Paramesvaran, A. Poll, S. Senkin, V.J. Smith, T. Williams

Rutherford Appleton Laboratory, Didcot, United Kingdom
K.W. Bell, A. Belyaev[49], C. Brew, R.M. Brown, D.J.A. Cockerill, J.A. Coughlan, K. Harder, S. Harper, E. Olaiya, D. Petyt, C.H. Shepherd-Themistocleous, A. Thea, I.R. Tomalin, W.J. Womersley, S.D. Worm

Imperial College, London, United Kingdom
M. Baber, R. Bainbridge, O. Buchmuller, D. Burton, D. Colling, N. Cripps, M. Cutajar, P. Dauncey, G. Davies, M. Della Negra, P. Dunne, W. Ferguson, J. Fulcher, D. Futyan, A. Gilbert,

G. Hall, G. Iles, M. Jarvis, G. Karapostoli, M. Kenzie, R. Lane, R. Lucas[48], L. Lyons, A.-M. Magnan, S. Malik, B. Mathias, J. Nash, A. Nikitenko[37], J. Pela, M. Pesaresi, K. Petridis, D.M. Raymond, S. Rogerson, A. Rose, C. Seez, P. Sharp†, A. Tapper, M. Vazquez Acosta, T. Virdee, S.C. Zenz

Brunel University, Uxbridge, United Kingdom
J.E. Cole, P.R. Hobson, A. Khan, P. Kyberd, D. Leggat, D. Leslie, W. Martin, I.D. Reid, P. Symonds, L. Teodorescu, M. Turner

Baylor University, Waco, USA
J. Dittmann, K. Hatakeyama, A. Kasmi, H. Liu, T. Scarborough

The University of Alabama, Tuscaloosa, USA
O. Charaf, S.I. Cooper, C. Henderson, P. Rumerio

Boston University, Boston, USA
A. Avetisyan, T. Bose, C. Fantasia, P. Lawson, C. Richardson, J. Rohlf, J. St. John, L. Sulak

Brown University, Providence, USA
J. Alimena, E. Berry, S. Bhattacharya, G. Christopher, D. Cutts, Z. Demiragli, N. Dhingra, A. Ferapontov, A. Garabedian, U. Heintz, G. Kukartsev, E. Laird, G. Landsberg, M. Luk, M. Narain, M. Segala, T. Sinthuprasith, T. Speer, J. Swanson

University of California, Davis, Davis, USA
R. Breedon, G. Breto, M. Calderon De La Barca Sanchez, S. Chauhan, M. Chertok, J. Conway, R. Conway, P.T. Cox, R. Erbacher, M. Gardner, W. Ko, R. Lander, T. Miceli, M. Mulhearn, D. Pellett, J. Pilot, F. Ricci-Tam, M. Searle, S. Shalhout, J. Smith, M. Squires, D. Stolp, M. Tripathi, S. Wilbur, R. Yohay

University of California, Los Angeles, USA
R. Cousins, P. Everaerts, C. Farrell, J. Hauser, M. Ignatenko, G. Rakness, E. Takasugi, V. Valuev, M. Weber

University of California, Riverside, Riverside, USA
K. Burt, R. Clare, J. Ellison, J.W. Gary, G. Hanson, J. Heilman, M. Ivova Rikova, P. Jandir, E. Kennedy, F. Lacroix, O.R. Long, A. Luthra, M. Malberti, H. Nguyen, M. Olmedo Negrete, A. Shrinivas, S. Sumowidagdo, S. Wimpenny

University of California, San Diego, La Jolla, USA
W. Andrews, J.G. Branson, G.B. Cerati, S. Cittolin, R.T. D'Agnolo, D. Evans, A. Holzner, R. Kelley, D. Klein, D. Kovalskyi, M. Lebourgeois, J. Letts, I. Macneill, D. Olivito, S. Padhi, C. Palmer, M. Pieri, M. Sani, V. Sharma, S. Simon, E. Sudano, Y. Tu, A. Vartak, C. Welke, F. Würthwein, A. Yagil

University of California, Santa Barbara, Santa Barbara, USA
D. Barge, J. Bradmiller-Feld, C. Campagnari, T. Danielson, A. Dishaw, K. Flowers, M. Franco Sevilla, P. Geffert, C. George, F. Golf, L. Gouskos, J. Incandela, C. Justus, N. Mccoll, J. Richman, D. Stuart, W. To, C. West, J. Yoo

California Institute of Technology, Pasadena, USA
A. Apresyan, A. Bornheim, J. Bunn, Y. Chen, J. Duarte, A. Mott, H.B. Newman, C. Pena, C. Rogan, M. Spiropulu, V. Timciuc, J.R. Vlimant, R. Wilkinson, S. Xie, R.Y. Zhu

Carnegie Mellon University, Pittsburgh, USA
V. Azzolini, A. Calamba, B. Carlson, T. Ferguson, Y. Iiyama, M. Paulini, J. Russ, H. Vogel, I. Vorobiev

University of Colorado at Boulder, Boulder, USA
J.P. Cumalat, W.T. Ford, A. Gaz, E. Luiggi Lopez, U. Nauenberg, J.G. Smith, K. Stenson, K.A. Ulmer, S.R. Wagner

Cornell University, Ithaca, USA
J. Alexander, A. Chatterjee, J. Chu, S. Dittmer, N. Eggert, N. Mirman, G. Nicolas Kaufman, J.R. Patterson, A. Ryd, E. Salvati, L. Skinnari, W. Sun, W.D. Teo, J. Thom, J. Thompson, J. Tucker, Y. Weng, L. Winstrom, P. Wittich

Fairfield University, Fairfield, USA
D. Winn

Fermi National Accelerator Laboratory, Batavia, USA
S. Abdullin, M. Albrow, J. Anderson, G. Apollinari, L.A.T. Bauerdick, A. Beretvas, J. Berryhill, P.C. Bhat, G. Bolla, K. Burkett, J.N. Butler, H.W.K. Cheung, F. Chlebana, S. Cihangir, V.D. Elvira, I. Fisk, J. Freeman, Y. Gao, E. Gottschalk, L. Gray, D. Green, S. Grünendahl, O. Gutsche, J. Hanlon, D. Hare, R.M. Harris, J. Hirschauer, B. Hooberman, S. Jindariani, M. Johnson, U. Joshi, K. Kaadze, B. Klima, B. Kreis, S. Kwan, J. Linacre, D. Lincoln, R. Lipton, T. Liu, J. Lykken, K. Maeshima, J.M. Marraffino, V.I. Martinez Outschoorn, S. Maruyama, D. Mason, P. McBride, P. Merkel, K. Mishra, S. Mrenna, Y. Musienko[29], S. Nahn, C. Newman-Holmes, V. O'Dell, O. Prokofyev, E. Sexton-Kennedy, S. Sharma, A. Soha, W.J. Spalding, L. Spiegel, L. Taylor, S. Tkaczyk, N.V. Tran, L. Uplegger, E.W. Vaandering, R. Vidal, A. Whitbeck, J. Whitmore, F. Yang

University of Florida, Gainesville, USA
D. Acosta, P. Avery, P. Bortignon, D. Bourilkov, M. Carver, T. Cheng, D. Curry, S. Das, M. De Gruttola, G.P. Di Giovanni, R.D. Field, M. Fisher, I.K. Furic, J. Hugon, J. Konigsberg, A. Korytov, T. Kypreos, J.F. Low, K. Matchev, P. Milenovic[50], G. Mitselmakher, L. Muniz, A. Rinkevicius, L. Shchutska, M. Snowball, D. Sperka, J. Yelton, M. Zakaria

Florida International University, Miami, USA
S. Hewamanage, S. Linn, P. Markowitz, G. Martinez, J.L. Rodriguez

Florida State University, Tallahassee, USA
T. Adams, A. Askew, J. Bochenek, B. Diamond, J. Haas, S. Hagopian, V. Hagopian, K.F. Johnson, H. Prosper, V. Veeraraghavan, M. Weinberg

Florida Institute of Technology, Melbourne, USA
M.M. Baarmand, M. Hohlmann, H. Kalakhety, F. Yumiceva

University of Illinois at Chicago (UIC), Chicago, USA
M.R. Adams, L. Apanasevich, V.E. Bazterra, D. Berry, R.R. Betts, I. Bucinskaite, R. Cavanaugh, O. Evdokimov, L. Gauthier, C.E. Gerber, D.J. Hofman, S. Khalatyan, P. Kurt, D.H. Moon, C. O'Brien, C. Silkworth, P. Turner, N. Varelas

The University of Iowa, Iowa City, USA
E.A. Albayrak[51], B. Bilki[52], W. Clarida, K. Dilsiz, F. Duru, M. Haytmyradov, J.-P. Merlo, H. Mermerkaya[53], A. Mestvirishvili, A. Moeller, J. Nachtman, H. Ogul, Y. Onel, F. Ozok[51], A. Penzo, R. Rahmat, S. Sen, P. Tan, E. Tiras, J. Wetzel, T. Yetkin[54], K. Yi

Johns Hopkins University, Baltimore, USA
B.A. Barnett, B. Blumenfeld, S. Bolognesi, D. Fehling, A.V. Gritsan, P. Maksimovic, C. Martin, M. Swartz

The University of Kansas, Lawrence, USA
P. Baringer, A. Bean, G. Benelli, C. Bruner, R.P. Kenny III, M. Malek, M. Murray, D. Noonan, S. Sanders, J. Sekaric, R. Stringer, Q. Wang, J.S. Wood

Kansas State University, Manhattan, USA
A.F. Barfuss, I. Chakaberia, A. Ivanov, S. Khalil, M. Makouski, Y. Maravin, L.K. Saini, S. Shrestha, N. Skhirtladze, I. Svintradze

Lawrence Livermore National Laboratory, Livermore, USA
J. Gronberg, D. Lange, F. Rebassoo, D. Wright

University of Maryland, College Park, USA
A. Baden, A. Belloni, B. Calvert, S.C. Eno, J.A. Gomez, N.J. Hadley, R.G. Kellogg, T. Kolberg, Y. Lu, M. Marionneau, A.C. Mignerey, K. Pedro, A. Skuja, M.B. Tonjes, S.C. Tonwar

Massachusetts Institute of Technology, Cambridge, USA
A. Apyan, R. Barbieri, G. Bauer, W. Busza, I.A. Cali, M. Chan, L. Di Matteo, V. Dutta, G. Gomez Ceballos, M. Goncharov, D. Gulhan, M. Klute, Y.S. Lai, Y.-J. Lee, A. Levin, P.D. Luckey, T. Ma, C. Paus, D. Ralph, C. Roland, G. Roland, G.S.F. Stephans, F. Stöckli, K. Sumorok, D. Velicanu, J. Veverka, B. Wyslouch, M. Yang, M. Zanetti, V. Zhukova

University of Minnesota, Minneapolis, USA
B. Dahmes, A. Gude, S.C. Kao, K. Klapoetke, Y. Kubota, J. Mans, N. Pastika, R. Rusack, A. Singovsky, N. Tambe, J. Turkewitz

University of Mississippi, Oxford, USA
J.G. Acosta, S. Oliveros

University of Nebraska-Lincoln, Lincoln, USA
E. Avdeeva, K. Bloom, S. Bose, D.R. Claes, A. Dominguez, R. Gonzalez Suarez, J. Keller, D. Knowlton, I. Kravchenko, J. Lazo-Flores, S. Malik, F. Meier, G.R. Snow, M. Zvada

State University of New York at Buffalo, Buffalo, USA
J. Dolen, A. Godshalk, I. Iashvili, A. Kharchilava, A. Kumar, S. Rappoccio

Northeastern University, Boston, USA
G. Alverson, E. Barberis, D. Baumgartel, M. Chasco, J. Haley, A. Massironi, D.M. Morse, D. Nash, T. Orimoto, D. Trocino, R.-J. Wang, D. Wood, J. Zhang

Northwestern University, Evanston, USA
K.A. Hahn, A. Kubik, N. Mucia, N. Odell, B. Pollack, A. Pozdnyakov, M. Schmitt, S. Stoynev, K. Sung, M. Velasco, S. Won

University of Notre Dame, Notre Dame, USA
A. Brinkerhoff, K.M. Chan, A. Drozdetskiy, M. Hildreth, C. Jessop, D.J. Karmgard, N. Kellams, K. Lannon, W. Luo, S. Lynch, N. Marinelli, T. Pearson, M. Planer, R. Ruchti, N. Valls, M. Wayne, M. Wolf, A. Woodard

The Ohio State University, Columbus, USA
L. Antonelli, J. Brinson, B. Bylsma, L.S. Durkin, S. Flowers, A. Hart, C. Hill, R. Hughes, K. Kotov, T.Y. Ling, D. Puigh, M. Rodenburg, G. Smith, B.L. Winer, H. Wolfe, H.W. Wulsin

Princeton University, Princeton, USA
O. Driga, P. Elmer, P. Hebda, A. Hunt, S.A. Koay, P. Lujan, D. Marlow, T. Medvedeva, M. Mooney, J. Olsen, P. Piroué, X. Quan, H. Saka, D. Stickland[2], C. Tully, J.S. Werner, A. Zuranski

University of Puerto Rico, Mayaguez, USA
E. Brownson, H. Mendez, J.E. Ramirez Vargas

Purdue University, West Lafayette, USA
V.E. Barnes, D. Benedetti, D. Bortoletto, M. De Mattia, L. Gutay, Z. Hu, M.K. Jha, M. Jones, K. Jung, M. Kress, N. Leonardo, D. Lopes Pegna, V. Maroussov, D.H. Miller, N. Neumeister, B.C. Radburn-Smith, X. Shi, I. Shipsey, D. Silvers, A. Svyatkovskiy, F. Wang, W. Xie, L. Xu, H.D. Yoo, J. Zablocki, Y. Zheng

Purdue University Calumet, Hammond, USA
N. Parashar, J. Stupak

Rice University, Houston, USA
A. Adair, B. Akgun, K.M. Ecklund, F.J.M. Geurts, W. Li, B. Michlin, B.P. Padley, R. Redjimi, J. Roberts, J. Zabel

University of Rochester, Rochester, USA
B. Betchart, A. Bodek, R. Covarelli, P. de Barbaro, R. Demina, Y. Eshaq, T. Ferbel, A. Garcia-Bellido, P. Goldenzweig, J. Han, A. Harel, A. Khukhunaishvili, G. Petrillo, D. Vishnevskiy

The Rockefeller University, New York, USA
R. Ciesielski, L. Demortier, K. Goulianos, G. Lungu, C. Mesropian

Rutgers, The State University of New Jersey, Piscataway, USA
S. Arora, A. Barker, J.P. Chou, C. Contreras-Campana, E. Contreras-Campana, D. Duggan, D. Ferencek, Y. Gershtein, R. Gray, E. Halkiadakis, D. Hidas, S. Kaplan, A. Lath, S. Panwalkar, M. Park, R. Patel, S. Salur, S. Schnetzer, S. Somalwar, R. Stone, S. Thomas, P. Thomassen, M. Walker

University of Tennessee, Knoxville, USA
K. Rose, S. Spanier, A. York

Texas A&M University, College Station, USA
O. Bouhali[55], A. Castaneda Hernandez, R. Eusebi, W. Flanagan, J. Gilmore, T. Kamon[56], V. Khotilovich, V. Krutelyov, R. Montalvo, I. Osipenkov, Y. Pakhotin, A. Perloff, J. Roe, A. Rose, A. Safonov, T. Sakuma, I. Suarez, A. Tatarinov

Texas Tech University, Lubbock, USA
N. Akchurin, C. Cowden, J. Damgov, C. Dragoiu, P.R. Dudero, J. Faulkner, K. Kovitanggoon, S. Kunori, S.W. Lee, T. Libeiro, I. Volobouev

Vanderbilt University, Nashville, USA
E. Appelt, A.G. Delannoy, S. Greene, A. Gurrola, W. Johns, C. Maguire, Y. Mao, A. Melo, M. Sharma, P. Sheldon, B. Snook, S. Tuo, J. Velkovska

University of Virginia, Charlottesville, USA
M.W. Arenton, S. Boutle, B. Cox, B. Francis, J. Goodell, R. Hirosky, A. Ledovskoy, H. Li, C. Lin, C. Neu, J. Wood

Wayne State University, Detroit, USA
C. Clarke, R. Harr, P.E. Karchin, C. Kottachchi Kankanamge Don, P. Lamichhane, J. Sturdy

University of Wisconsin, Madison, USA
D.A. Belknap, D. Carlsmith, M. Cepeda, S. Dasu, L. Dodd, S. Duric, E. Friis, R. Hall-Wilton, M. Herndon, A. Hervé, P. Klabbers, A. Lanaro, C. Lazaridis, A. Levine, R. Loveless, A. Mohapatra, I. Ojalvo, T. Perry, G.A. Pierro, G. Polese, I. Ross, T. Sarangi, A. Savin, W.H. Smith, D. Taylor, P. Verwilligen, C. Vuosalo, N. Woods

†: Deceased
1: Also at Vienna University of Technology, Vienna, Austria
2: Also at CERN, European Organization for Nuclear Research, Geneva, Switzerland
3: Also at Institut Pluridisciplinaire Hubert Curien, Université de Strasbourg, Université de Haute Alsace Mulhouse, CNRS/IN2P3, Strasbourg, France
4: Also at National Institute of Chemical Physics and Biophysics, Tallinn, Estonia
5: Also at Skobeltsyn Institute of Nuclear Physics, Lomonosov Moscow State University, Moscow, Russia
6: Also at Universidade Estadual de Campinas, Campinas, Brazil
7: Also at Laboratoire Leprince-Ringuet, Ecole Polytechnique, IN2P3-CNRS, Palaiseau, France
8: Also at Joint Institute for Nuclear Research, Dubna, Russia
9: Also at Suez University, Suez, Egypt
10: Also at Cairo University, Cairo, Egypt
11: Also at Fayoum University, El-Fayoum, Egypt
12: Also at British University in Egypt, Cairo, Egypt
13: Now at Sultan Qaboos University, Muscat, Oman
14: Also at Université de Haute Alsace, Mulhouse, France
15: Also at Brandenburg University of Technology, Cottbus, Germany
16: Also at Institute of Nuclear Research ATOMKI, Debrecen, Hungary
17: Also at Eötvös Loránd University, Budapest, Hungary
18: Also at University of Debrecen, Debrecen, Hungary
19: Also at University of Visva-Bharati, Santiniketan, India
20: Now at King Abdulaziz University, Jeddah, Saudi Arabia
21: Also at University of Ruhuna, Matara, Sri Lanka
22: Also at Isfahan University of Technology, Isfahan, Iran
23: Also at Sharif University of Technology, Tehran, Iran
24: Also at Plasma Physics Research Center, Science and Research Branch, Islamic Azad University, Tehran, Iran
25: Also at Università degli Studi di Siena, Siena, Italy
26: Also at Centre National de la Recherche Scientifique (CNRS) - IN2P3, Paris, France
27: Also at Purdue University, West Lafayette, USA
28: Also at Universidad Michoacana de San Nicolas de Hidalgo, Morelia, Mexico
29: Also at Institute for Nuclear Research, Moscow, Russia
30: Also at St. Petersburg State Polytechnical University, St. Petersburg, Russia
31: Also at California Institute of Technology, Pasadena, USA
32: Also at Faculty of Physics, University of Belgrade, Belgrade, Serbia
33: Also at Facoltà Ingegneria, Università di Roma, Roma, Italy
34: Also at Scuola Normale e Sezione dell'INFN, Pisa, Italy
35: Also at University of Athens, Athens, Greece
36: Also at Paul Scherrer Institut, Villigen, Switzerland
37: Also at Institute for Theoretical and Experimental Physics, Moscow, Russia
38: Also at Albert Einstein Center for Fundamental Physics, Bern, Switzerland
39: Also at Gaziosmanpasa University, Tokat, Turkey
40: Also at Adiyaman University, Adiyaman, Turkey

41: Also at Cag University, Mersin, Turkey
42: Also at Anadolu University, Eskisehir, Turkey
43: Also at Izmir Institute of Technology, Izmir, Turkey
44: Also at Necmettin Erbakan University, Konya, Turkey
45: Also at Ozyegin University, Istanbul, Turkey
46: Also at Marmara University, Istanbul, Turkey
47: Also at Kafkas University, Kars, Turkey
48: Also at Rutherford Appleton Laboratory, Didcot, United Kingdom
49: Also at School of Physics and Astronomy, University of Southampton, Southampton, United Kingdom
50: Also at University of Belgrade, Faculty of Physics and Vinca Institute of Nuclear Sciences, Belgrade, Serbia
51: Also at Mimar Sinan University, Istanbul, Istanbul, Turkey
52: Also at Argonne National Laboratory, Argonne, USA
53: Also at Erzincan University, Erzincan, Turkey
54: Also at Yildiz Technical University, Istanbul, Turkey
55: Also at Texas A&M University at Qatar, Doha, Qatar
56: Also at Kyungpook National University, Daegu, Korea